AGU PUBLICATIONS

JGR

Journal of Geophysical Research: Earth Surface

RESEARCH ARTICLE
10.1002/2016JF004132

Key Points:
- Tidal notch modeling incorporating Holocene sea level, erosion rates, and landmass movement
- Optically emphasized morphological consequences of biasing slow and rapid coastal displacements
- Resulting notch sequences do not necessarily link to certain seismic events and are not chronologically sorted

Supporting Information:
- Supporting Information S1
- Movie S1
- Movie S2
- Movie S3
- Movie S4
- Movie S5
- Movie S6
- Movie S7
- Movie S8
- Movie S9
- Movie S10

Correspondence to:
S. Schneiderwind,
s.schneiderwind@nug.rwth-aachen.de

Citation:
Schneiderwind, S., S. J. Boulton, I. Papanikolaou, M. Kázmér, and K. Reicherter (2017), Numerical modeling of tidal notch sequences on rocky coasts of the Mediterranean Basin, *J. Geophys. Res. Earth Surf.*, *122*, doi:10.1002/2016JF004132.

Received 3 NOV 2016
Accepted 25 APR 2017
Accepted article online 28 APR 2017

Numerical modeling of tidal notch sequences on rocky coasts of the Mediterranean Basin

S. Schneiderwind[1], S. J. Boulton[2], I. Papanikolaou[3], M. Kázmér[4,5], and K. Reicherter[1]

[1]Institute of Neotectonics and Natural Hazards, RWTH Aachen University, Aachen, North Rhine-Westphalia, Germany, [2]School of Geography, Earth and Environmental Sciences, Plymouth University, Plymouth, UK, [3]Laboratory of Mineralogy and Geology, Agricultural University of Athens, Athens, Greece, [4]Department of Palaeontology, Eötvös University, Budapest, Hungary, [5]Now at MTA-ELTE Geological, Geophysical and Space Science Research Group, Eötvös University, Budapest, Hungary

Abstract Tidal notches have had the potential to form at sea level from ~6.5 kyr B.P. in the Mediterranean Basin and preserve a symmetrical shape comparable to a quadric polynomial. Continuous erosion, predominantly by biological agents, affects a limestone cliff face from low- to high-tide level at <1 mm/yr. Statically determined, the roots of a quadric polynomial are defined by the tidal range representing the limits of effective erosion. However, gradual variations of eustatic sea level rise (slow) and coseismic uplift/subsidence (fast) in tectonically active regions contribute to vertical shifts in the erosional base at coastlines. As a consequence, the cliff morphology gets modified through time resulting in widening, deepening, and separation of notches and possible overprinting of older features. In order to investigate successive modifications of coastal cliff morphology, we developed a numerical model that considers the erosion rate, the erosion zone relative to sea level, the regional sea level curve, and tectonic motion. The results show how slow and rapid sea level changes bias the modern cliff face and highlight that the present-day notch sequence from top descending to sea level is not inevitably of decreasing age. Furthermore, the initiation of notch formation is not necessarily linked to the date of a certain seismic event. Especially in extensional tectonic settings where coseismic uplift is low and coastal morphological marks are not as distinct, knowledge about coastal evolution is beneficial for paleoseismological research.

1. Introduction

Tidal notches are a generally accepted sea level marker [e.g., *Pirazzoli et al.*, 1982, 1989, 1991; *Laborel et al.*, 1999; *Kershaw and Guo*, 2001; *Evelpidou et al.*, 2011a, 2011ab, 2012a, 2012a; *Boulton and Stewart*, 2015; *Antonioli et al.*, 2015]. Ongoing horizontal erosion of chemical, physical, and biological agents [e.g., *Furlani et al.*, 2011; *Antonioli et al.*, 2015; *Evelpidou and Pirazzoli*, 2016] contributes to notch formation at mean sea level. As a result, obvious ecological and morphological topographies that range from a few centimeters up to several meters deep occur predominantly on limestone coastlines where tidal ranges are low and erosional processes are concentrated into a narrow vertical range of elevation [*Pirazzoli*, 1986]. It is generally assumed, when these features are raised or submerged from present-day sea level, that paleo-historic tectonic activity can be inferred from obtained sequences. In particular, tidal notches along coasts of the Mediterranean Sea have been an important marker of coastal tectonism determining rates of Holocene tectonic uplift [e.g., *Pirazzoli et al.*, 1982, 1989, 1991, 1994, *Stewart and Vita-Finzi*, 1996; *Rust and Kershaw*, 2000; *Kershaw and Guo*, 2001; *Evelpidou et al.*, 2012a, *Antonioli et al.*, 2015; *Goodman-Tchernov and Katz*, 2015] (Figure 1). However, it remains unclear as to what present morphologies can reveal regarding the paleomagnitudes and coseismic uplift of historic earthquakes. It is generally assumed that tidal notches form during relative sea level stagnation, when vertical land movements and eustatic trends are unison. The database of *Boulton and Stewart* [2015] demonstrated that the formation of tidal notches is not linked to periods of stable or unstable climates in the past, rather it is likely that tectonic activity and earthquake clustering control the spatial and temporal distributions of tidal notches. Only rapid offset between the strandline and erosional base can initiate new notch generation. Thus, the distinction between surface displacement potential in compressional and extensional tectonic settings is absolutely essential [*Schneiderwind et al.*, 2017]. Yet coseismic offsets on normal faults are at least an order of magnitude smaller than those from thrusting events. However, the misconception that multiple and stacked notches are evidence for meter-scale coseismic events produced by normal faulting still persists [e.g., *Stewart and Vita-Finzi*, 1996]. Therefore, *Cooper et al.* [2007] suggest a different mechanism to explain the occurrence of meter-scale shoreline

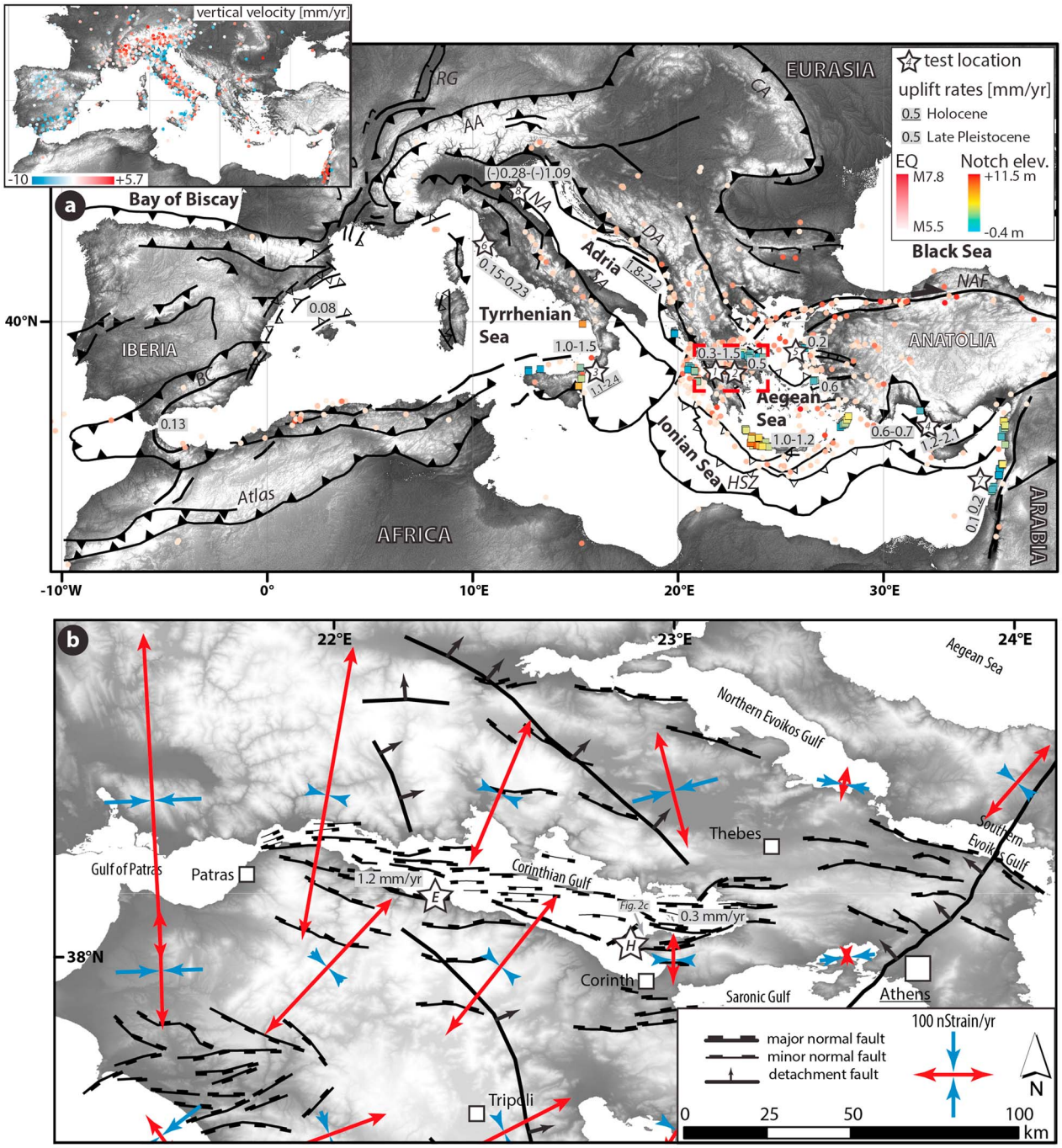

Figure 1. Study areas throughout the Mediterranean. (a) Plate tectonic setting of the Mediterranean [modified after *Faccenna et al.*, 2014]. Inset shows vertical motion velocity derived from continuous GPS stations provided by *Serpelloni et al.* [2013]. Obvious coherent patterns of uplift (e.g., Alps) and subsidence (e.g., Spain) demonstrate the tremendous diversity of the Mediterranean geodetic field. *Boulton and Stewart* [2015] provided a database on tidal notches (rectangles) in the eastern Mediterranean Basin. Estimates on regional and local uplift rates range across from −1.09 to 2.4 mm/yr [*Collier et al.*, 1992; *Westaway*, 1993; *Stewart and Vita-Finzi*, 1996; *Stewart et al.*, 1997; *Zazo et al.*, 1999; *Stiros et al.*, 2000; *Sivan et al.*, 2001; *Leeder et al.*, 2003; *Zazo et al.*, 2003; *Lambeck et al.*, 2004; *McNeill and Collier*, 2004; *Westaway et al.*, 2004; *Antonioli et al.*, 2006; *Cooper et al.*, 2007; *Ferranti et al.*, 2007; *Carcaillet et al.*, 2009; *Roberts et al.*, 2009; *Cundy et al.*, 2010; *Schildgen et al.*, 2012; *Roberts et al.*, 2013; *Harrison et al.*, 2013]. The stars indicate test regions: (1) western Gulf of Corinth, (2) eastern Gulf of Corinth, (3) eastern Sicily and Calabria, (4) southern margin of the central Anatolian Plateau, (5) Samos Island, (6) Tuscan coast, (7) Carmel Coast, and (8) northern Adriatic. Earthquake (EQ) data covering <500 events (1905–2015) with a maximum focal depth of 20 km are provided by the U.S. Geological Survey. AA = Alpine Arc, DA = Dinaric Alps, CA = Carpathian Arc, BC = Betic Cordilleras, HSZ = Hellenic Subduction Zone, NA = Northern Adriatic, NAF = North Anatolian Fault, RG = Rhine Graben. (b) Geodynamics of central Greece. Faults were compiled from *Koukouvelas et al.* [1996], *Papanikolaou and Papanikolaou* [2007], *Papanikolaou and Royden* [2007], *Sakellariou et al.* [2007], *Roberts et al.* [2009], and *Grützner et al.* [2016]. Strain rates are from *Hollenstein et al.* [2008]. The stars indicate the location of the test sites for model comparison with actual cliff faces from the Eliki fault (E) and Cape Heraion (H) The red box indicates extents of Figure 1b.

displacements along normal faults, proposing that individual notches formed when stable climate facilitated sustained erosion and postglacial sea level rise became outpaced by the coastal uplift rate. Contrasting this suggestion, *Boulton and Stewart* [2015] argue that this hypothesis does not seem to be the case for the Mediterranean and conclude that notch genesis is dominantly controlled by earthquake clustering.

Only a few attempts to model tidal notch formation have been undertaken. Conceptual notch formation is understood as a reflection of normal distributed erosional potential resulting in a symmetrical shape with the retreat zone of maximum convexity at mean sea level. *Pirazzoli* [1986] developed the generally accepted idea of a symmetrical V-/U-shaped notch profile on a sheltered cliff where the floor extends to the limit of permanent immersion at tidal lowstand, and the roof marks the upper limit of frequent high tides. The maximum retreat point is located near mean sea level. Gradual relative sea level change may produce a variety of tidal notch profiles. *Evelpidou et al.* [2011a, 2011b] provided a set of graphic schemes of tidal notch profiles resulting from different combinations of relative sea level changes. In general, the authors pointed out that relative sea level stability deepens the notch whereas gradual sea level change widens the morphological incision. Furthermore, rapid sea level changes can be divided into two categories: first where rapid relative movements greater than the tidal range result in notch formation while the former notch remains preserved and second rapid displacements smaller than the tidal range that produce notch profiles with two closely located vertices separated by a small protrusion in between. In other words, the preexisting morphology is modified due to overlapping erosional zones prior to and after the displacement [see also *Pirazzoli*, 1986; *Evelpidou et al.*, 2012a]. Notch profile modification is also a product of increasing exposure to wave action. Other than bioerosive agents, cliff quarrying by wave action is generally not considered in tidal notch development. It is generally assumed that quarrying is insignificant for sheltered exposures [*Pirazzoli*, 1986; *Antonioli et al.*, 2015]. However, *Larson et al.* [2011] introduced an analytical, yet physically based, model that considers wave impacts on coastal dunes and cliffs from laboratory experiments. Their results show complex feedback in cliff notch evolution when nearby beaches provide sediments that increase the erosive capacity of impacting waves. A third approach is presented by *Trenhaile* [2014] focusing on notch formation by tidal wetting and drying cycles and salt weathering. Here notch profiles were produced within the 3000–6000 year period of constant relative sea level. As a result of ongoing erosion affecting the same cliff section, several iterative cliff collapses were generated. Wetting and drying cycles as well as salt weathering attain importance especially when saline water penetrates into structural discontinuities of the bedrock. Evaporation processes and subsequent cumulative deposition of salt crystals trigger fragmentation of the rock and result in geomorphic modifications. A similar process occurs owing to frost weathering in cold climates [*Trenhaile and Mercan*, 1984]. By applying a gridded mathematical model *Trenhaile* [2016] suggests for limestone notch profiles in the Mediterranean that notch morphology is the product of a variety of local- (e.g., cliff slope and bed resistance to erosion) and regional-scale (e.g., varying erosional efficacy) factors. By adding a wide range of different variables (e.g., variable slope gradient and notch collapse on a local scale and general influence of sea level changes on a regional scale) a theoretical approach is provided suggesting that similar profiles can be produced by different combinations of applied parameters.

Except for the work of *Trenhaile* [2015], all previous notch models do not address actual changing glacio-hydro-isostatic conditions during the Holocene. Although previous studies generally consider changing sea levels, both rapid and gradual, unlocking the temporal interplay between sea level change causative factors has not yet been deeply investigated. However, considering actual and region-specific parameters enhances the understanding of the development of paleoshorelines and their deformation by active tectonics particularly for paleoseismological studies. Therefore, previous models are herein described as static (theoretical) models. In order to visualize the development of notch sequences incorporating eustatic and isostatic balances, erosion rates, coseismic uplift, and cliff steepness, we present a simple numerical model that simulates the migration of the erosional base through the Holocene. Furthermore, local sea level curves and coastal uplift rates for eight regions across the Mediterranean Basin act as input parameters in order to verify potentials of notch formation and associated theoretical paleoseismological significance when earthquake activity is introduced as well. Both slow and rapid relative landmass displacements interplay through time causing overprinting and modification of preexisting notch generations. As the first application in this manner, the time-sliced visualization enables researchers to have an enhanced understanding of tidal notch sequence evolution, and thus better interpretations of coseismic sequences on tectonic coasts.

2. Contributors to Notch Sequencing

The term tidal notch refers to a horizontal erosion feature at sea level [*Kelletat*, 2005b] due to the coeval action [*Antonioli et al.*, 2015] of biological, chemical, and physical factors [*Pirazzoli*, 1986]. It should be noted that the ratio between erosional components has not been discovered so far. *Pirazzoli and Evelpidou* [2013] consider only tidal notches that exclusively formed by bioerosional processes in sheltered places, and other workers have similarly concluded that biological mechanisms at least dominate notch forming erosion potentials [*Evelpidou et al.*, 2012b; *Antonioli et al.*, 2015]. Referring to bioerosion, it is generally assumed that horizontal galleries of coring and boring organisms, frequently submerged by periodic tides, are most active in the midlittoral zone that extends across the tidal range [e.g., *Pirazzoli*, 1986; *Evelpidou et al.*, 2012a]. Thereby, sheltered and vertical exposures are promising locations for the preservation of symmetrical sea level markers.

Antonioli et al. [2015] point out that salt weathering, wetting and drying cycles, the potential of karst dissolution, and wave action also play important roles in notch formation. The occurrence of a spray zone in more exposed sites introduces a physiochemical erosion component in terms of salt weathering, where the deposition of salt crystals and hydration will modify the notch shape. *Porter et al.* [2010] demonstrated that intertidal wetting and drying and salt weathering are also possible. Dependent on the frequency and duration of tidal immersion and exposure intervals, periods for salt crystallization within cracks and fissures are formed supporting this type of haloclastic weathering. Chemical erosion through the dissolution of carbonates is not a common effect of seawater exposure, which is (over) saturated with $CaCO_3$ [*Kelletat*, 2005b]. The content of calcium carbonate may be lowered only in very localized coastal sections next to springs that show evidence of solution by effluent groundwater [*Evelpidou et al.*, 2012b]. Indeed, nearby freshwater sources support karst dissolution and therefore increase the erosion rate [*Evelpidou et al.*, 2015; *Evelpidou and Pirazzoli*, 2016]. The vulnerability to different types of physical erosion on coastal cliffs is influenced by the resistance of the rock to wave attack, which is a function of lithology and structural discontinuities, such as cracks, fissures, joints, bedding planes, and faults [e.g., *Kershaw and Guo*, 2001; *Trenhaile*, 2014, 2015]. The rock is even more affected when turbulent water contains air that gets compressed when smashed against the rock and causes cavitation pitting [*Antonioli et al.*, 2015]. However, cliff collapses are rare for Mediterranean limestone coastlines [*Trenhaile*, 2016]. Thick-bedded neritic limestones support the overburden and hence the preservation of decimeter-scale deep incisions (Figure 2). Furthermore, most of these Mesozoic limestones are often not deformed by tectonics; e.g., the massive Parnassos and Gavrovo-Tripolis Units crossing the Corinthian Gulf in central Greece comprise of 1.5–3 km thick neritic mostly undeformed limestones [e.g., *Papanikolaou*, 1984; *Papanikolaou and Royden*, 2007].

As a function of the erosion rate, the period of balanced eustatic sea level rise and isostatic regional uplift controls how deep an indentation develops. However, eustasy, isostasy, and vertical tectonic movements exhibit considerable spatial and temporal variabilities throughout the Holocene [*Lambeck et al.*, 2004] (Figure 1). *Boulton and Stewart* [2015] compared local sea level curves with associated regional uplift estimates and concluded that the highest-elevation tidal notch on uplifting coasts should date to ~6000 years B.P. Not until that time did the rate of eustatic sea level rise decrease to ~1 mm/yr and reach gravitational equilibrium with the continental lithosphere [*Carminati et al.*, 2003; *Stocchi et al.*, 2005]. In his modeling approach *Trenhaile* [2016] concludes that notches develop as long as sea level change is no greater than 5.6 mm/yr. For the Mediterranean, sea level rise decreased to this rate ~6800 years ago. Subsequently, slow relative sea level changes have caused gradual changes of the erosional base at emerging coastlines.

By contrast, discrete notch levels record abrupt shoreline changes caused by local seismic displacements. In order to preserve the shape and fragile intertidal fauna, rapid removal from the tidal zone and lift beyond the reach of waves is needed [*Boulton and Stewart*, 2015]. However, in rifting regions shallow normal faulting events of $M \leq 7$ commonly produce coseismic uplift limited to a few decimeters along the footwall of the causative fault. Along such faults the uplift/subsidence ratio is estimated to be 1/2 to 1/4 of net slip per event [e.g., *Stewart and Vita-Finzi*, 1996; *Armijo et al.*, 1996; *McNeill et al.*, 2005; *Papanikolaou et al.*, 2010]. Even in microtidal environments, such as the Mediterranean Sea, rapid displacements due to coseismic uplift most likely do not exceed the tidal range.

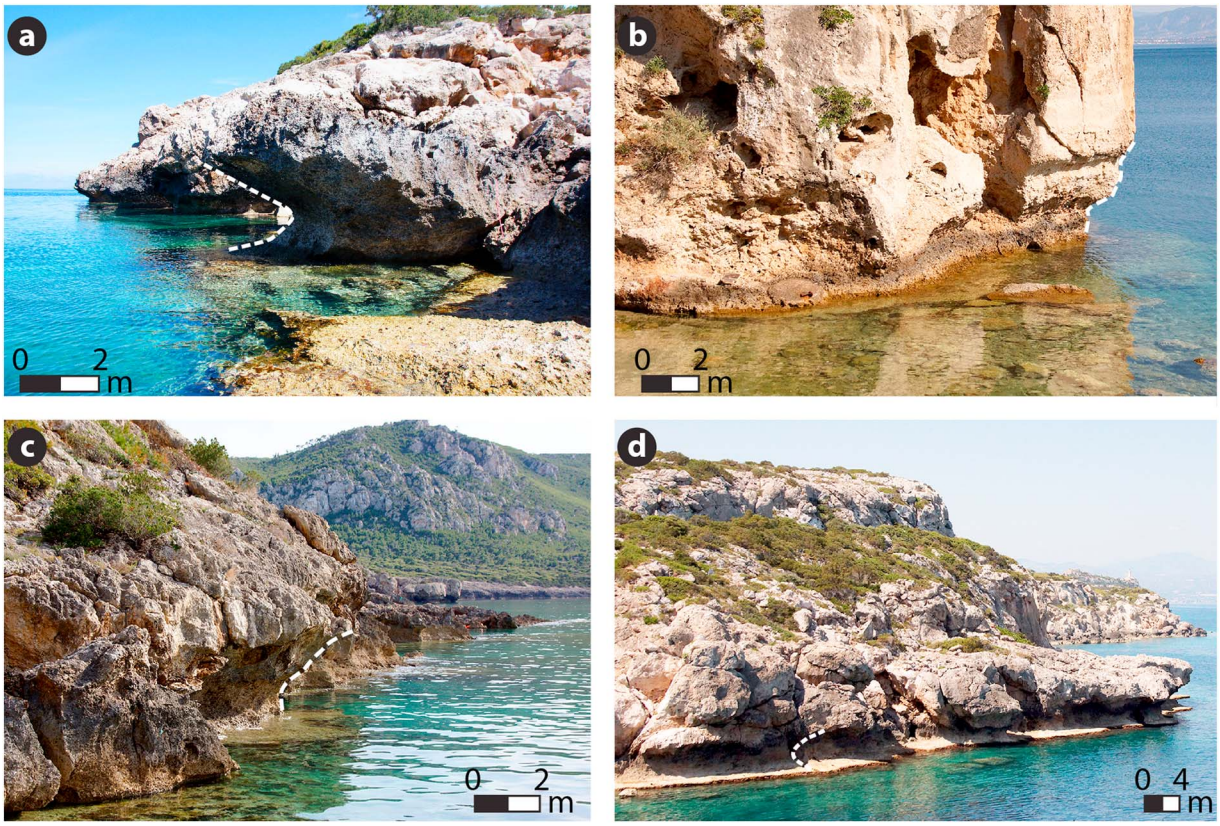

Figure 2. Examples for deeply incised notches withstanding cliff collapse in the Mediterranean. Thick-bedded Triassic-Lower Jurassic neritic limestones belonging to the Beotia Unit along the coast of the Perachora Peninsula (eastern Corinthian Gulf, Greece) can support the overburden even when incised up to ~2 m. Profiles are indicated by white dashed lines. (a and d) Raised shorelines closely located to Cape Heraion. (b) A sequence of different raise shorelines also at Cape Heraion. (c) Incised Cliff at Sterna (see Figure 1b).

Therefore, as a consequence of both, slow and rapid variations in the position of the erosional base, notch shape modification occurs. To distinguish between notch widening and new notch development is challenging (Figure 3). It has to be expected that the time period for notch formation might be short and the resulting indentation is only of minor scale and that massive overprinting and degradation of older features have occurred since ~6000 years B.P.

In order to evaluate stagnation and shifting of the erosional base projected on a present-day cliff face, the long-term geodetic motion should be considered. However, the vertical component of the Mediterranean geodetic field varies dramatically. Continuous GPS stations all over Europe highlight the presence of spatially coherent patterns of uplift and subsidence (Figure 1). *Serpelloni et al.* [2013] presented up to 14 years of vertical GPS ground motion rates for the Mediterranean region. Their results show that the fastest subsidence of ~ -3 mm/yr is located in southern Spain, while general uplift (~2 mm/yr) is obtained for the Alps. Furthermore, the data set indicates landmass uplift of ~1 mm/yr toward the eastern part of the Mediterranean Basin, such as for the island of Crete and the Cyclades. However, the network density here is significantly lower than in central Europe; thus, the vertical deformation is less well constrained for the eastern Mediterranean. In addition, the precision of vertical positions determined by most GPS station is ~1 mm/yr [*Serpelloni et al.*, 2013; *Faccenna et al.*, 2014] and observation periods are small in comparison to geological timescales [*Papanikolaou et al.*, 2005].

Long-term Quaternary activity is generally reflected in coastal geomorphology, including uplifted Pleistocene marine terraces and notches of Holocene age in steep calcareous cliffs. Benefits of dating such features are that they represent approximations of cumulative rates over multiple seismic cycles [*McNeill and Collier*, 2004]. Nevertheless, variations in vertical movements across the Mediterranean region are also presented by several studies (Figure 1). For the western Mediterranean only very minor uplift rates are obtained [e.g., *Zazo et al.*, 1999, 2003]. In the central region, predominantly concentrated at

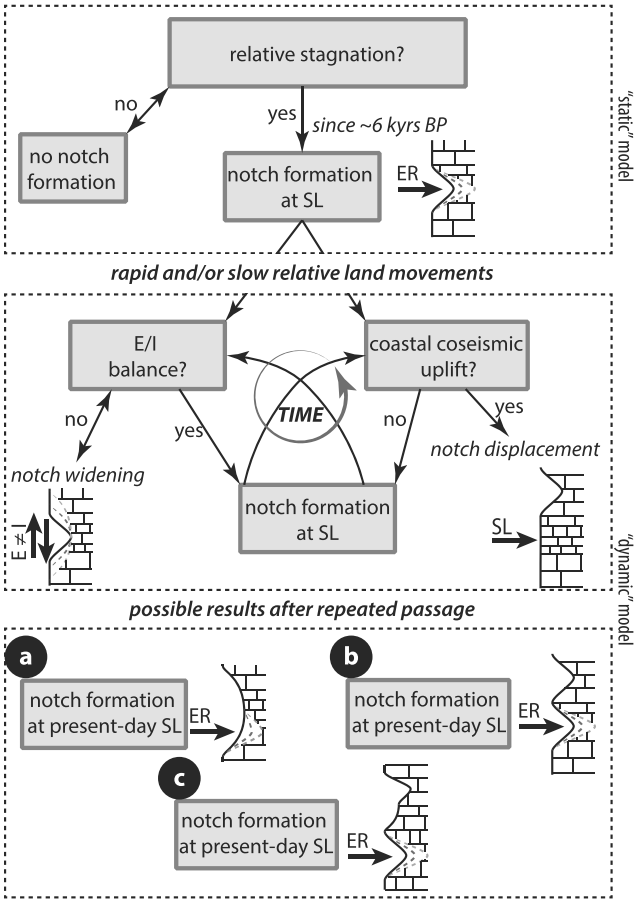

Figure 3. Logic tree for tidal notch sequence evolution. The static notch formation model incorporates only the erosion rate (ER) to estimate the notch depth. The dynamic model considers gradual sea level (SL) changes due to unbalanced eustasy (E) and isostasy (I), and coseismic land displacements. Resulting cliff shapes contain (a) widened notches, (b) emerged notches, or (c) a combination of all that.

the coastlines of Sicily and southern Italy, several studies have been undertaken calculating uplift rates ranging from 1.0 to 2.4 mm/yr [e.g., *Westaway*, 1993; *Stewart et al.*, 1997; *Antonioli et al.*, 2006]. The rapidly extending Corinthian Gulf produces Holocene uplift rates of 0.3 mm/yr in the eastern parts up to 1.5 mm/yr in the most western parts [e.g., *Stewart and Vita-Finzi*, 1996; *Leeder et al.*, 2003; *Cooper et al.*, 2007]. While close to the Hellenic Subduction Zone (HSZ) *Roberts et al.* [2013] calculated an average uplift rate of 1.0–1.2 mm/yr derived from marine terraces at the island of Crete. For the southern margin of the central Anatolian Plateau (CAP) estimates for Holocene uplift range from 0.6 to 0.7 mm/yr [*Schildgen et al.*, 2012]. By contrast, the Levantine coastline is assumed to be tectonically stable for the past 10 ka [e.g., *Sivan et al.*, 2001, 2004; *Goodman-Tchernov and Katz*, 2015].

3. Dynamic Notch Formation

In the first instance, the rate of relative sea level change determines whether a tidal notch will develop or not. For the Mediterranean, estimates of limestone erosion rates range from 0.2 top 1.0 mm/yr [*Pirazzoli and Evelpidou*, 2013; *Evelpidou and Pirazzoli*, 2016]. Thus, balanced conditions between eustasy and isostasy have to persist for about 200 years to develop a significant 20 cm deep notch. The notch height would approximately equal the tidal range for which estimates range from 0.3 to 0.4 m for the majority of the Mediterranean [*Evelpidou et al.*, 2012b; *Evelpidou and Pirazzoli*, 2016], although exceptional tides of up to 1.8 m may occur in the northern Adriatic [*Trenhaile*, 2016]. Shape modification is given by exposure and/or organic accretions [*Pirazzoli*, 1986; *Antonioli et al.*, 2015]. Increasing exposure yields an upward shifted roof while the base remains at low tide level. Thus, the height of a notch is primarily controlled by exposure to wave action. Biological accretions are located at the base of a notch. If present the lower part of the notch is no longer a mirrored copy of the upper part but reduced in size. However, a simplified description is supported by sheltered conditions and the absence of biological accretions. Then, the coefficients of a quadric polynomial can cover the requirements to describe such symmetrical shapes (Figure 4). As in a conceptual static model, notch depth is specified by erosion rate (mm/yr) × time (yr) of a constant erosional base.

The dynamic model (considering actual relative sea level change; Figure 3) calculates the parabolic erosion for every year considering both rapid and slow relative sea level changes and computes the cumulative sum of erosional impacts. Using a local sea level curve and information regarding ongoing isostatic and dated coseismic uplift as inputs to control the migration of the erosional base enables us to describe the vertical cliff morphology at a given moment.

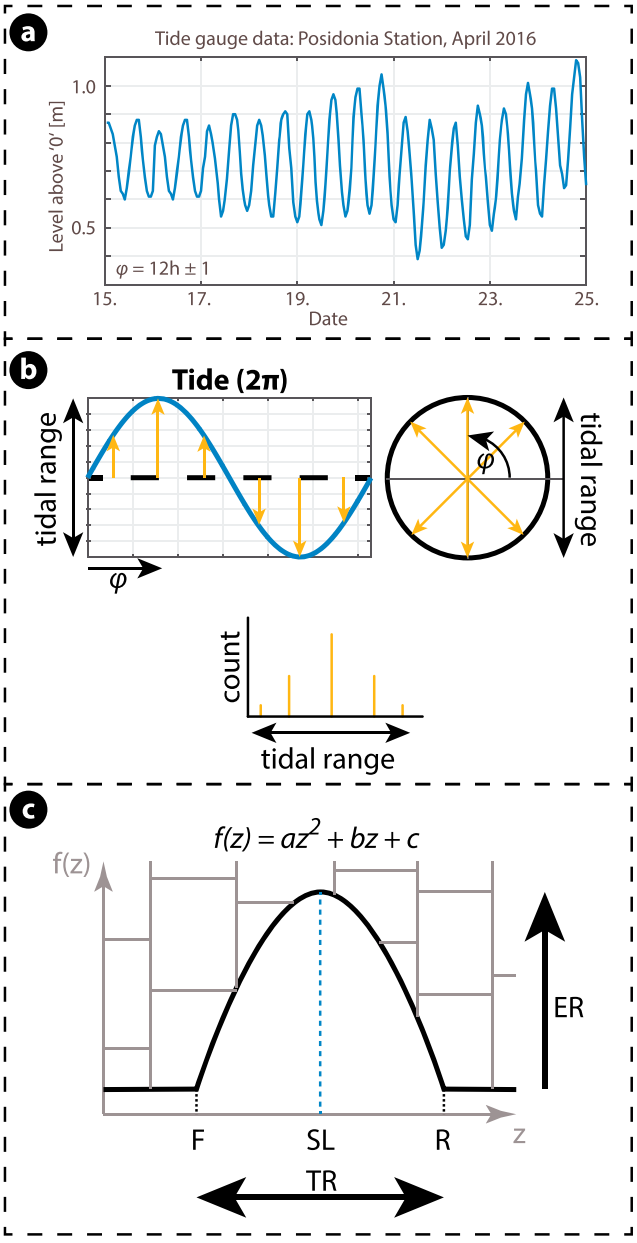

Figure 4. Assumptions leading to a quadric polynomial to cover requirements of tidal notch shape description: (a) actual tide gauge data from April 2016 for the eastern Gulf of Corinth provided by the Hellenic Navy Hydrographic Service. The φ is the tide period. (b) The diurnal tide equals a sine function in a long-term average. Plotted into an unit cycle the moment φ depicts an angle pointing to an associated height within the tidal range. Each height depicts a bin in the histogram plot. (c) A quadric polynomial describing the depth $f(z)$ along a symmetrical notch profile. Floor (F) and roof (R) depict the roots separated by the tidal range (TR) along the x axis. Note, the x axis is labeled as "z" for a better understanding since it represents the vertical orientation of the cliff face. The erosion rate (ER) corresponds to c and determines the depth of the notch after 1 year.

4. Methodology

The modeling algorithm developed here incorporates eustatic and isostatic balances, erosion rates, cliff steepness, and coseismic uplift. Therefore, the input parameters that have to be specified for the model are (i) the tidal range (m), (ii) the erosion rate (m/yr), (iii) a long-term coastal uplift rate (mm/yr) and eustatic information [e.g., *Lambeck and Purcell*, 2005], and (iv) the average steepness of the cliff in degrees. Values of coseismic uplifts (m) from one or more events are optional but have to be linked to a number of years B.P. if given.

The initial conditions in the model are characterized by an infinite cliff. The influences of the cliff slope are widely discussed in *Pirazzoli* [1986] (Figure 3) yielding in asymmetrical notch shapes when different from a straight 90° [see also *Trenhaile*, 2016]. In order to run predictions from the most favorable conditions [*Pirazzoli*, 1986] the initial setting corresponds to situations where the cliff is vertical.

Following the static model idea, notch development occurs at sea level and does not change through time. The depth $d(z)$ of the notch at different stages is expressed as a quadric polynomial as follows:

$$d(z) = az^2 + bz + ER \times dt \quad (1)$$

where the coefficients a, b, and ER define the codomain and shape of the graph in accordance to the erosional base. The erosion rate (ER) provokes a translation in y direction and represents the eroded depth after 1 year (dt) at mean sea level. The parameter b is the gradient at the y axis. However, when mean sea level is set to zero the inflection point is located at the y axis. Hence, the gradient b is zero. The curvature at the inflection point is defined by a. Thereby, the roots at floor and roof, respectively, act as targets the graph has to pass. Since these are given by the extents of the tidal range, they can be utilized to transcribe a as a function of the erosion rate as follows:

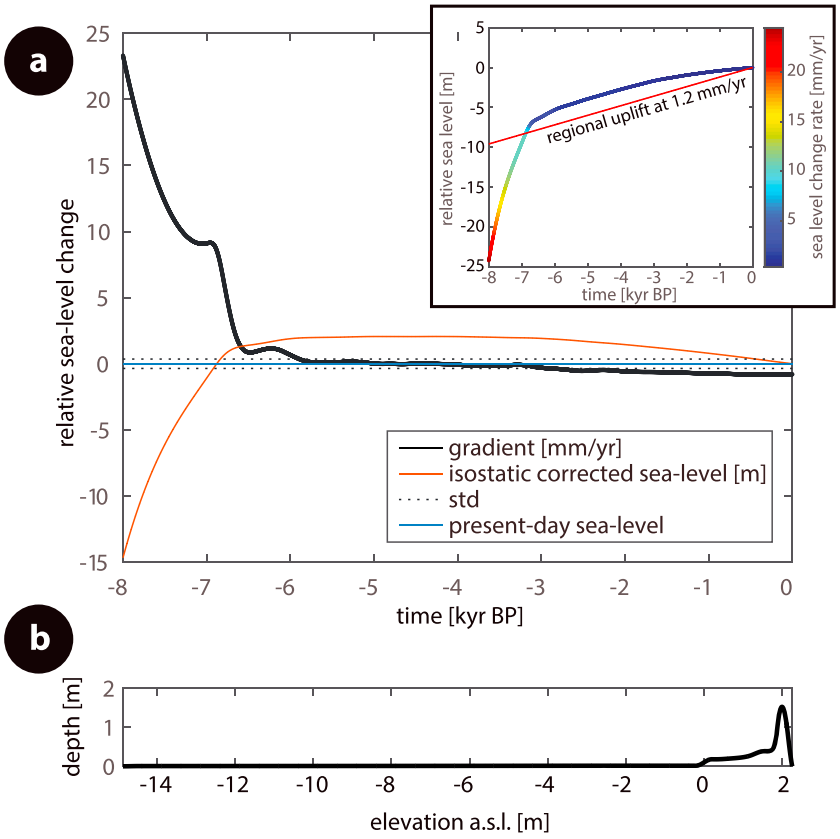

Figure 5. Applied sea level curve and coastal uplift (inset graph) resulting in tidal notches: (a) sea level curve [e.g., *Lambeck and Purcell*, 2005] corrected for coastal uplift; (b) resulting notch sequence.

$$a = \frac{f(z)}{(eb - z_{s1}) \times (eb - z_{s2})} \tag{2}$$

Here $f(z)$ is the determined depth in succession of 1 year of penetrating erosion. Parameter *eb* depicts mean sea level and is set to zero. The roots z_{s1} and z_{s2} represent the floor and the roof of the notch and hence obtain values of half the tidal range with different sign.

In order to consider the change of the erosional base through the Holocene, the difference between a given sea level curve and applied coastal uplift is included. When correcting a sea level curve for the isostatic trend, the time of notch formation is indicated for periods where the gradient is ~0 (Figure 5a). Afterward, the Cartesian grid is translated for every year, so that the origin always equals the erosional base. Thereby, the grid translation circumvents complex recalculations of *a*. Indeed, the result is an examination per year. Therefore, a matrix (size: elevation, years B.P.) is generated incorporating the cumulative sums of each simulated profile. Consequently, the last array of the matrix represents the modeled notch sequence covering the entire vertical extent of affected parts during the simulation. Furthermore, by calculating the erosional base it is also demonstrated that the erosive zone does not project below −3 m (Figure 6). We assume that this is shallow enough to exclude larger-scale morphologies such as continuously submerged shore platforms from the model.

The purpose of this paper is to simulate vertical coastal cliff evolution during the late Holocene visualizing the interplay between slow and rapid regional-scale contributors to changes in erosional efficacy. Therefore, the model is simplified, refraining notch shape influencing parameters such as wetting and drying cycles and salt weathering, predicting vertical cliff profiles only for sites with high potentials of tidal notch development and preservation. Following the suggestions from *Pirazzoli* [1986], cliffs sheltered from wave action located in a microtidal environment pose ideal sites for tidal notch development with a minimum of shape modification and best preconditions for tidal notch preservation. For the central and eastern Mediterranean low-moderate

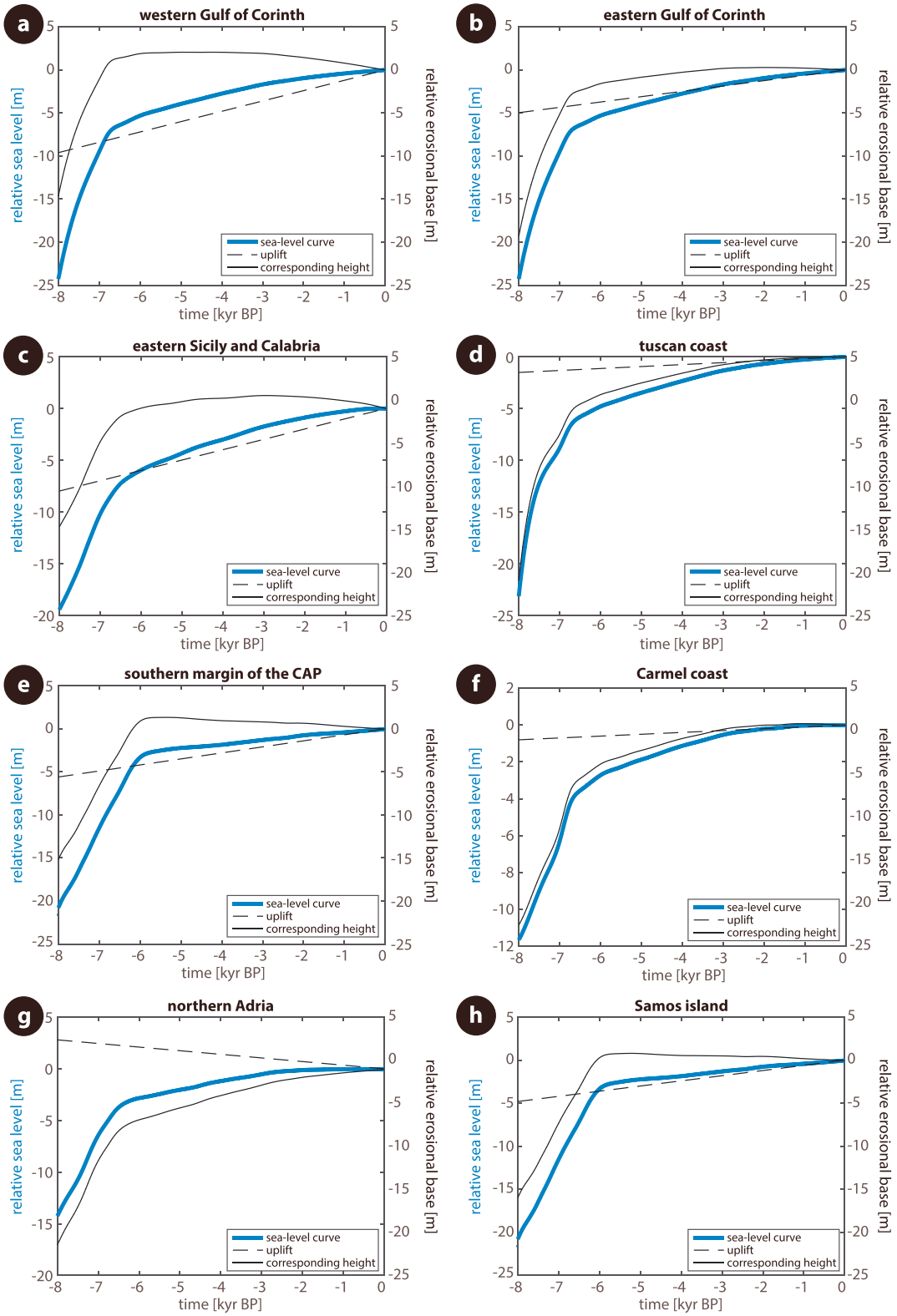

Figure 6. Sea level curves and uplift trend-corrected erosional bases corresponding to todays' sea level datum. (a–c) Regions in Greece and Italy experience >1 mm/yr coastal uplift. (d–f and h) These regions represent areas of minor uplift. (g) The northern Adriatic coast has continuously subsided since the Last Glacial Maximum.

wave energy potentials with mean values around 6–7 kW/m are presented in *Besio et al.* [2016]. Altimeter significant wave height measurements suggest mean values of ~1 m for the entire Mediterranean Basin [*Queffeulou and Bentamy*, 2007]. In calm and semienclosed subbasins within the Mediterranean, such as the Tyrrhenian coast, the northern Adriatic, the Ionian Aegean Sea, and the Levantine coast, wave heights are up to 0.6 m with wave periods of around 1–5 s [e.g., *Ayat*, 2013; *Liberti et al.*, 2013]. Furthermore, we are referring to tidal notches which do not have to be confused with other marine notches formed by sediment abrasion. Closely located sediment sources such as beaches and strong currents may support the development of such abrasional notches, which do not necessarily correspond to the tidal range. Moreover, the amount of bioerosion is minimized in such grinding environments [*Kelletat*, 2005b]. An important condition for tidal notch preservation is the bedrock lithology. Databases on tidal notches in the Mediterranean [e.g., *Boulton and Stewart*, 2015] show that they mostly occur in neritic thick-bedded or even massive limestones. Besides that cliff collapse is uncommon in the Mediterranean [*Trenhaile*, 2016] due to lithological conditions (see Figure 2), considering cliff failure is irrelevant for decoding the cliff evolution of an actual cliff where preserved paleostrandlines can be observed.

5. Results

In order to demonstrate how sensitive the algorithm is for differing input parameters and how diverse notch development occurs through time we applied local conditions of eight different regions across the Mediterranean to the algorithm (Table 1). Furthermore, coseismic activity is included in the model for two specific sites (Figure 1b and Table 2).

5.1. Uplifting Coastal Regions: Western/Eastern Gulf of Corinth and Eastern Sicily and Calabria

The mid-Holocene sea level curve for the Peloponnese coast (Greece) from *Lambeck and Purcell* [2005] shows a monotonically increasing sea level and does not contain characteristics such as a mid-Holocene highstand or punctuated parts (Figures 6a and 6b). At ~7000 yr B.P. the rate of sea level change decreases considerably and potentially forms conditions for relative sea level stagnation at ~6000 years B.P., when applying an average coastal uplift of 1.2 mm/yr [*De Martini et al.*, 2004]. After correcting the curve for the uplift trend, the resulting gradient allows the timing of notch development to be described (see Figures 3 and 5a). The result of 7000 years of a vertically shifting erosional base is shown in Figure 7. Almost 6.8 kyr B.P. notch formation begins and corresponds to a 15 cm deep notch ~1.4 m above present-day sea level. A minor variation and sea level rise of ~6.1 kyr B.P. yield an upward shift of the erosional base. Not until 5.9 kyr B.P. is the next equilibrium is reached. During the period in between an upward grazing occurs which indicates that the rate of sea level change is still slow enough to significantly erode the limestone. From 5.9 to 2.6 kyr B.P., a period of almost no sea level change occurs at a corresponding height of ~2 m resulting in an indentation of almost 1.5 m depth and ~0.4 m height, at an erosion rate of 0.5 mm/yr. The subsequent gradual and slow lowering of the erosional base until present-day sea level produces and overprints the first stage of notch formation. From a present-day view a notch appears at ~1.5 m which is actually the result of two erosional phases 6.5 kyr and 2.5 kyr B.P., respectively. It should be noted that the first period yields in a 15 cm deep notch that gets heavily overprinted by the second phase. To conclude cliff morphology evolution for the western Gulf of Corinth, an entire sequence of three notches at ~2 m, ~1.5 m, and present-day sea level can develop without any rapid vertical motion of the strandline.

The same sea level curve forms the input for the eastern Gulf of Corinth simulation. The highest extensional rates of up to 15 mm/yr are estimated for the western part of the Gulf. Long-term vertical movements toward the Alkyonides Gulf are lower; where a net uplift rate of 0.7 mm/yr is applied following estimates of *Stewart and Vita-Finzi* [1996] [see also *Roberts et al.*, 2009]. The resultant modeled cliff section is markedly different to that predicted for the western Gulf of Corinth. The trend-corrected sea level curve does not reach its stagnation phase, where the gradient is almost zero, until ~3 kyr B.P. (Figure 6b). However, at ~6.8 kyr B.P. the rate of change is small enough so that the erosive potential penetrates almost the same area over a considerable time period at a corresponding height of −1.9 m. Gradual vertical shifts during the period between ~6.2 and 6 kyr B.P. graze the rock no deeper than 0.1 m but across ~1 m in height. Hereafter, the rate of sea level change decreases again increasing the penetration time and supporting the development notch of a small notch. At ~5 kyr B.P. a third decrease in sea level gradient occurs, but which is still faster than the 0.7 mm/yr uplift. Corresponding to today's sea level the erosional zone is located −0.5 m during that stage (Figure 7b)

Table 1. Applied Input Parameters for Different Regions[a]

	SLC	Tidal Range	Vertical Motion	EQ?	Erosion Rate	Cliff
W. Gulf of Corinth, Greece	*Lambeck and Purcell* [2005]	0.3 m	(+) 1.2 mm/yr	no	0.5 mm/yr	90°
E. Gulf of Corinth, Greece	*Lambeck and Purcell* [2005]	0.3 m	(+) 0.6 mm/yr	no	0.5 mm/yr	90°
E. Sicily and Calabria, Italy	*Lambeck et al.* [2004]	0.3 m	(+) 1.0 mm/yr	no	0.5 mm/yr	90°
Tuscan Coast, Italy	*Lambeck and Purcell* [2005]	0.3 m	(+) 0.2 mm/yr	no	0.5 mm/yr	90°
S. margin of the CAP, Turkey	*Lambeck* [1995]	0.3 m	(+) 0.7 mm/yr	no	0.5 mm/yr	90°
Carmel Coast, Israel	*Lambeck and Purcell* [2005]	0.3 m	(+) 0.1 mm/yr	no	0.5 mm/yr	90°
N. Adria, Italy	*Lambeck et al.* [2004]	0.3 m	(−) 0.35 mm/yr	no	0.5 mm/yr	90°
Samos Island, Greece	*Lambeck* [1995]	0.3 m	(+) 0.6 mm/yr	no	0.5 mm/yr	90°

[a]SLC = source of the sea level curve. CAP = central Anatolian Plateau.

and shifts to the present datum ~3.8 kyr B.P. Subsequently, a fourth stage of a lowered sea level change gradient causes an increasing indentation at a corresponding height of ~0.2 m. However, very minor gradual changes widen the developing notch. The stagnation is then reached ~3 kyr B.P. This phase lasts for ~2000 years ending up in a final stage of gentle lowering the erosional base. The last 1000 years are dominated by forming the present-day tidal notch of >1 m depth that overwrites preexisting erosive structures.

The sea level curve for the north-western part of the Ionian Sea also has two main periods of rising sea level. The transition between both is not as clear as for the Gulf of Corinth, but ~6.5 kyr B.P. sea level rise stopped outpacing an uplift of ~1.0 mm/yr [*Westaway*, 1993; *Tortorici et al.*, 1995; *Stewart et al.*, 1997; *Ferranti et al.*, 2007]. When the sea level curve is corrected for this uplift trend, the erosional base has two minor rising steps at ~5 kyr and 3.5 kyr B.P., respectively (Figure 6c). The highest erosional level of ~2 m dates to ~3 kyr B.P. before it decreases to present-day sea level. A more detailed view is given by corresponding time slices in Figure 8. Incision into the cliff began 6.4 kyr B.P. when the rate of sea level rise decreased significantly. However, not until 5.5 kyr B.P. is the gradient low enough to form a distinct indentation at a corresponding height of ~0.4 m. The penetration period lasts ~600 years when a gradual upward shift of the erosive base for ~0.5 m occurs, resulting in a widening of the indentation. Around 4.8 kyr B.P. the erosion occurs at a corresponding height of ~0.9 m and forms a notch of ~0.5 m depth at 0.8 m above sea level (asl). Subsequently, another upward shift ~3.3 kyr B.P. causes a third distinct indentation at ~1.2 m asl. An equilibrium state for >1000 years yields not only in a resulting notch depth of up to 0.8 m but also overwrites the roof topography of the underlying notch. During the period between 1.8 kyr B.P. and 1 kyr B.P. successive lowering of the erosional base causes a downward widening of the latest indentation and erosion of former notch topographies. The subsequent stage is dominated by grazing the cliff downward and again of overprinting structures that formed ~4500 years earlier. Today, the erosive sequence shows three to four notches

Table 2. Input of Coseismic Parameter (Dates in Bold Numbers)[a]

	No.	Elevation (m)	Dated to	Coseismic Uplift (m)
Heraion, Perachora Peninsula	1	3.2	**4380** ± 60 B.P.	0.6
	2	2.6	**2350** ± 90 B.P.	0.9
	3	1.7	ND (**1333** B.P.)	0.6
	4	1.1	**315** ± 125 B.P.	1.1
Eliki, w. Gulf of Corinth	1	–	ND (**7352** B.P.)	0.25
	2	–	ND (**6643** B.P.)	0.2
	3	–	ND (**5934** B.P.)	0.3
	4	–	ND (**5225** B.P.)	0.28
	5	–	ND (**4516** B.P.)	0.22
	6	–	ND (**3807** B.P.)	0.25
	7	–	ND (**3098** B.P.)	0.22
	8	3.7	2290 ± 115 B.P.2600 ± 265 B.P.**2389** B.P.	0.23
	9	1.8	**1680** ± 130 B.P.	0.25
	10	–	ND (**831** B.P.)	0.26
	11	–	**89** B.P.	0.26

[a]*Pirazzoli et al.* [1994] dated three notches at Heraion and identified a fourth generation at 1.7 m (asl). *Stewart and Vita-Finzi* [1996] dated two shorelines at the Eliki fault in the western Gulf of Corinth and estimated 0.2–0.3 m coseismic uplift per event.

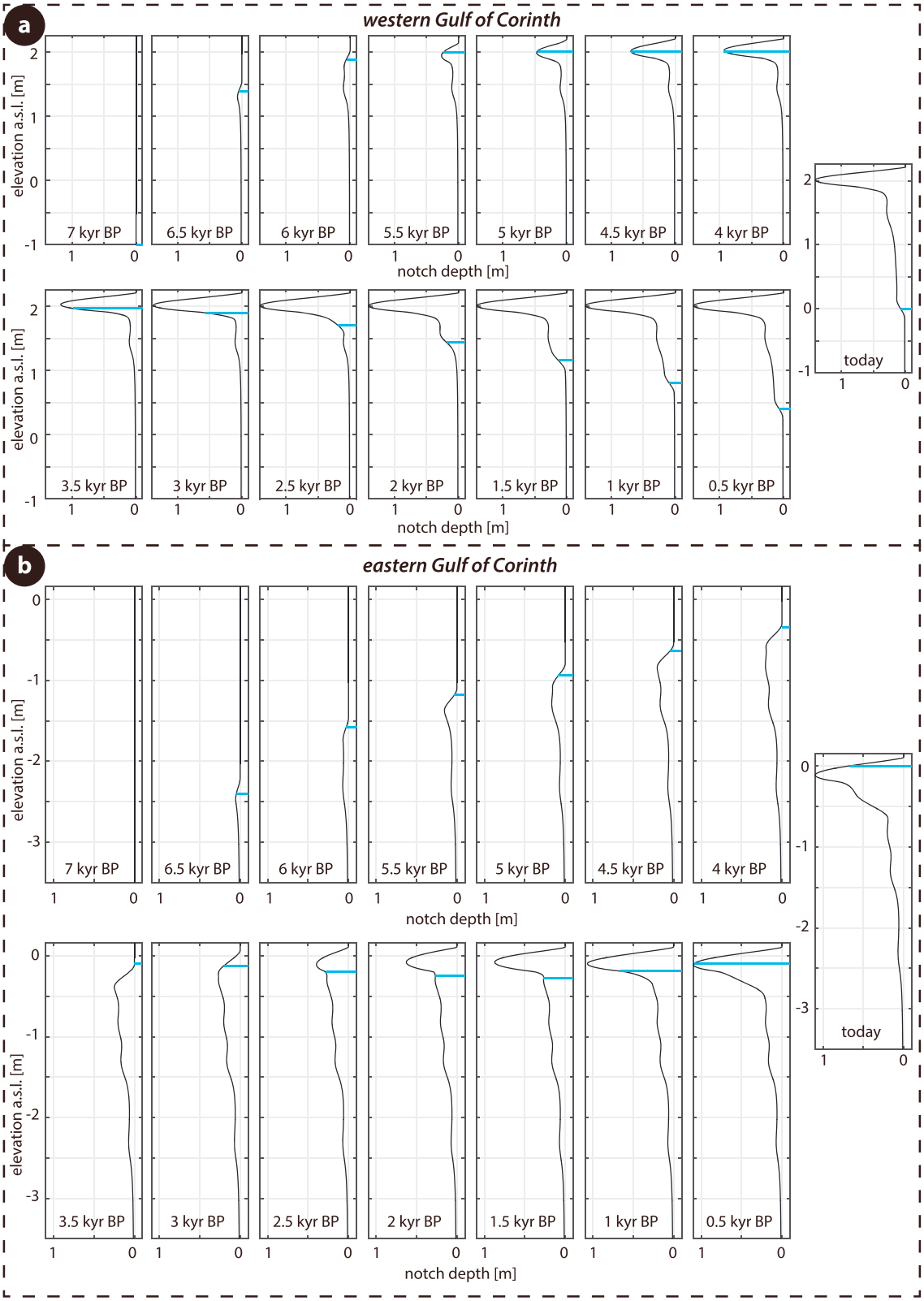

Figure 7. Time slices of tidal notch development on rapidly emerging coastlines such as the (a) western Gulf of Corinth and its (b) eastern part accompanied by moderate emergence. The blue lines indicate sea level at that time.

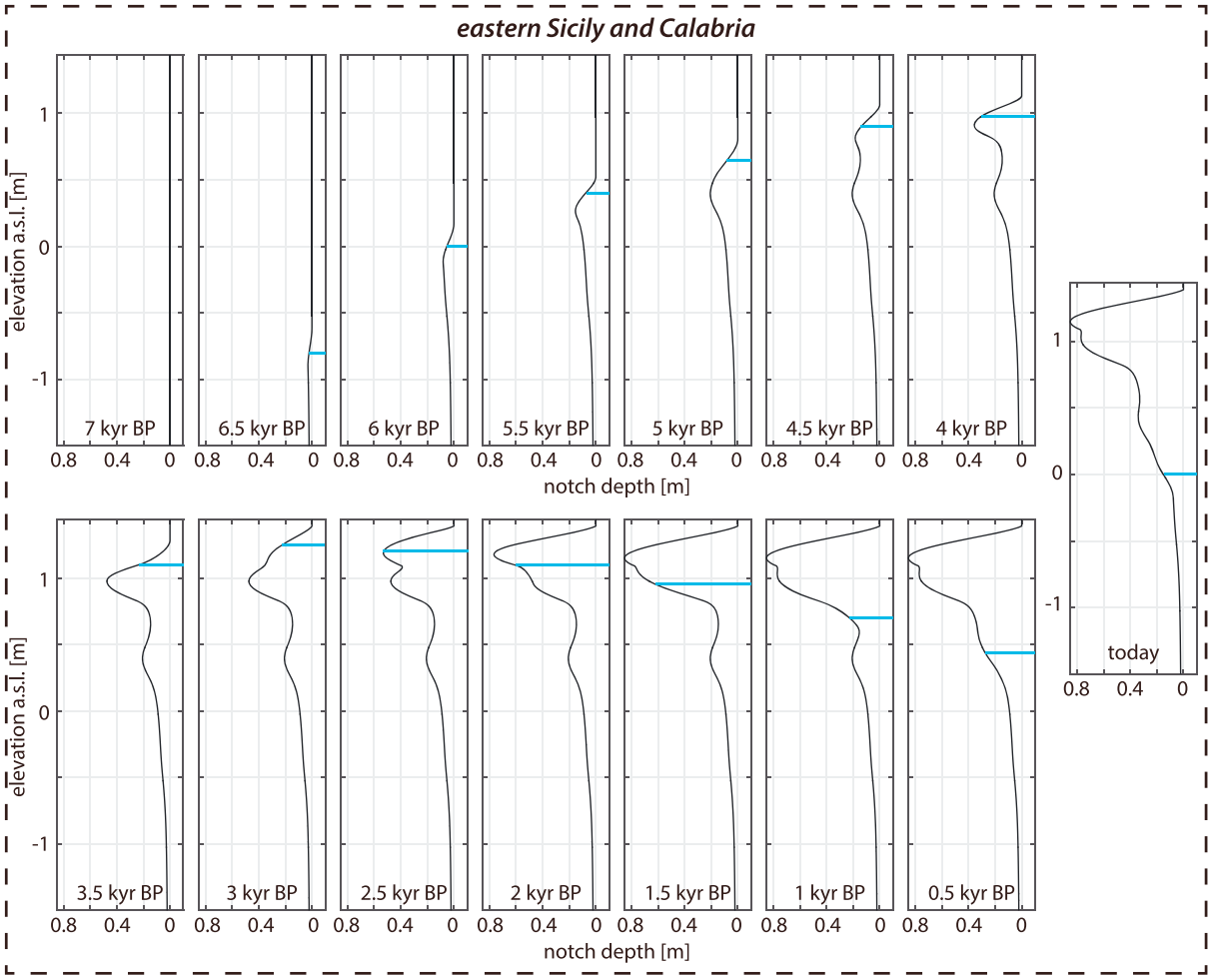

Figure 8. Simulated notch formation time slices for eastern Sicily and Calabria which pose examples for moderately emerging coasts. The blue lines indicate sea level at that time.

(+1.2, +1.0, +0.4, and currently forming), which match up with elongated periods of relative sea level stagnation, but their depths are heavily altered during grazing phases.

5.2. Moderately Uplifting Coastal Regions: Southern Turkey and Eastern Aegean Sea

For the southern margin of the central Anatolian Plateau (CAP, southern Turkey) uplift at 0.7 mm/yr was estimated by *Schildgen et al.* [2012]. This rate slightly outpaces the local sea level curve within the period of the last 6000 years. However, the rising rate of sea level change is characterized by very minor variations so that the corresponding erosional base evenly decreases from ~1.4 m to the present datum (Figures 6e and 9a). The development of the cliff morphology is characterized by distinct notch formation for about 1500 years from 6 to 4.5 kyr B.P., subsequent lowering of the erosional base resulting in extensive downward grazing, and again focused notch formation at ~0.7 m from 4–2.5 kyr B.P., removing the floor of the earlier feature. A subsequent minor shift of ~0.1 m causes a third indentation just below the last. The present-day notch is the result of gradual down-shifting the erosional base.

By contrast, a distinct knickpoint forms at ~6 kyr B.P. along the coast of Samos Island (Figure 6h) where the net uplift is estimated at 0.6 mm/yr [*Stiros et al.*, 2000], which is comparatively low but matches the overall rate of sea level rise for the last 6000 years. Consequently, notch development occurs along a very narrow horizon for the mid-Holocene period (Figure 9b). Ongoing erosive penetration against the cliff appears at ~5.8 kyr B.P. resulting in a notch of ~0.7 m depth at a corresponding height of 0.7 m. A minor shift of ~0.2 m toward todays' datum causes distinct notch formation from 3.5 to 1.5 kyr B.P. The present-day tidal notch forms during the last 1000 years, resulting in a single composite notch.

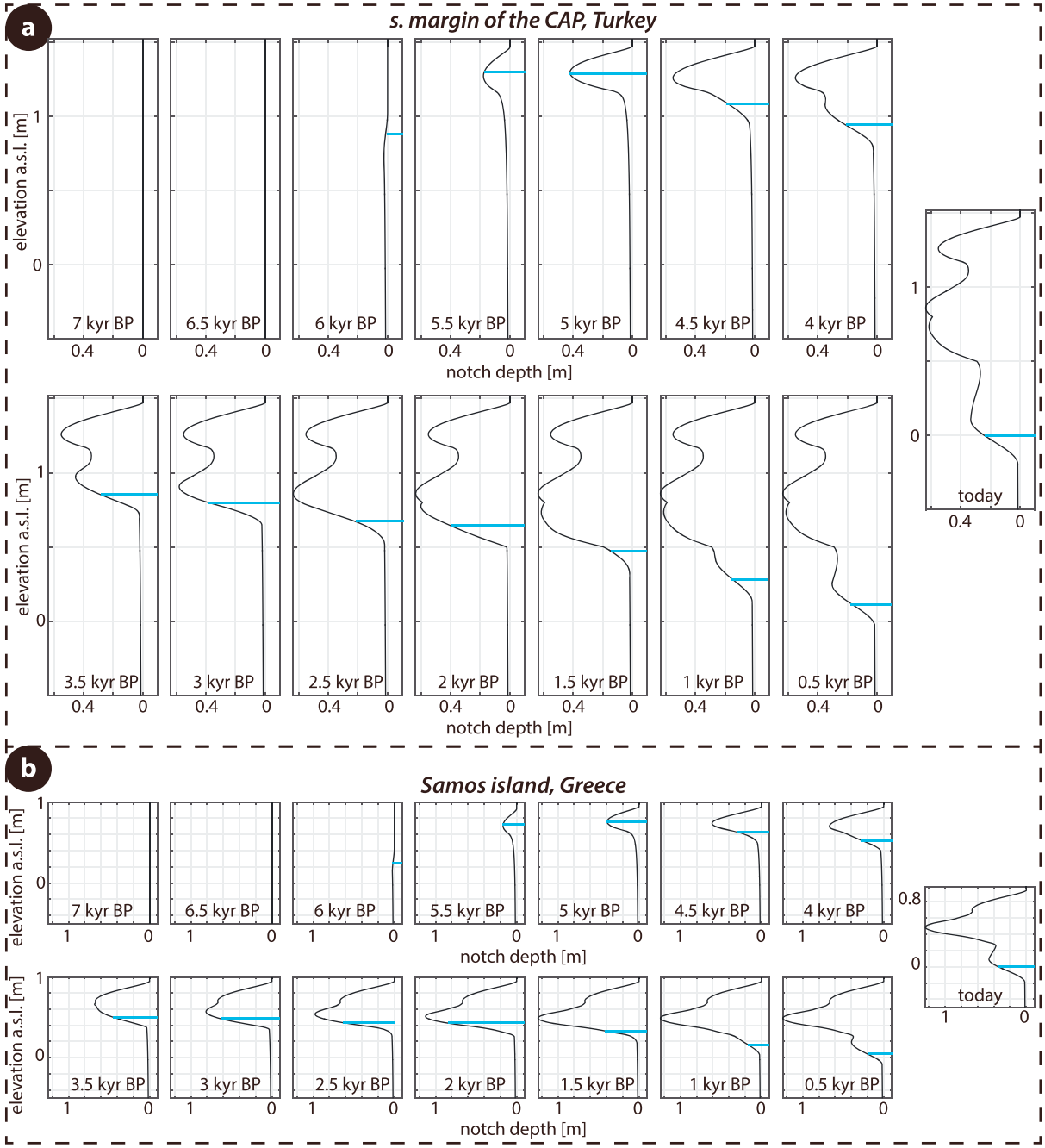

Figure 9. Time slices from tidal notch simulation in (a) southern Turkey and in the (b) eastern Aegean Sea. Both regions are representative for coastlines emerging at significantly less than 1 mm/yr. The blue lines indicate sea level at that time.

5.3. Tectonically Stable Regions: Tuscan Coast and Carmel Coast

A short period (7.5–7 kyr B.P.) of lower rates of sea level rise followed by again steep rising before sea level change adjusts at a moderate slope ~6.5 kyr B.P. is the most characteristic part of the Tuscan coast mid-Holocene sea level curve (Figure 6d). *Lambeck et al.* [2004] stated that the shorelines along the northern and central Thyrrenian coasts are largely free from vertical tectonic movements and uplift is only at 0.2 mm/yr in the Holocene interval. Therefore, trend correction to estimate the erosional base has only a minor influence on rates of sea level change. Potentially, tidal notch development initiates 2.9 kyr B.P. without further noteworthy vertical changes. From the time slices (Figure 10) it is obvious that considerable grazing of

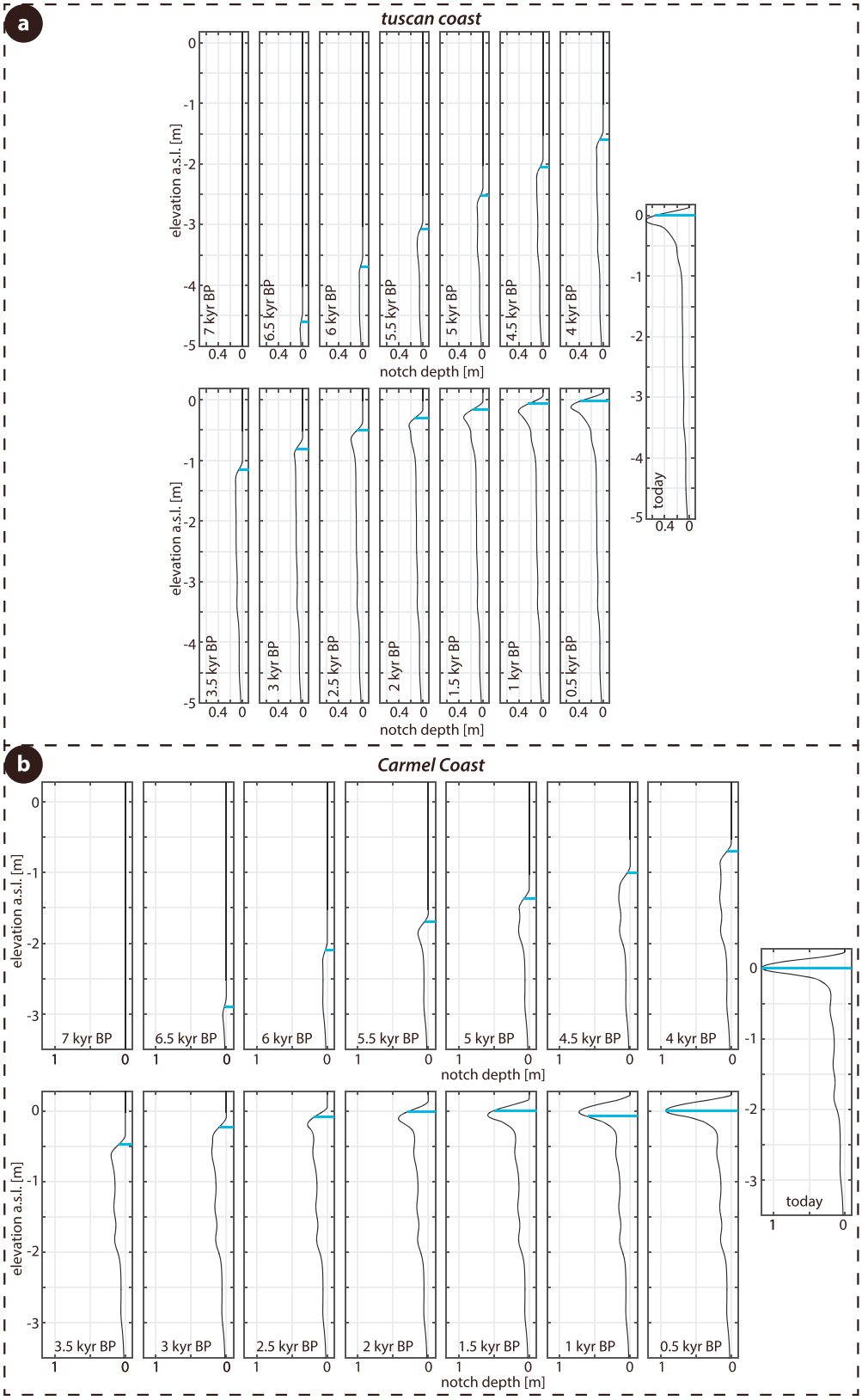

Figure 10. Time slices of mid-Holocene notch development in tectonically stable regions. (a) Northern Thyrrenian Sea, coast of Tuscany. (b) Carmel Coast, Isreal. The blue lines indicate sea level at that time.

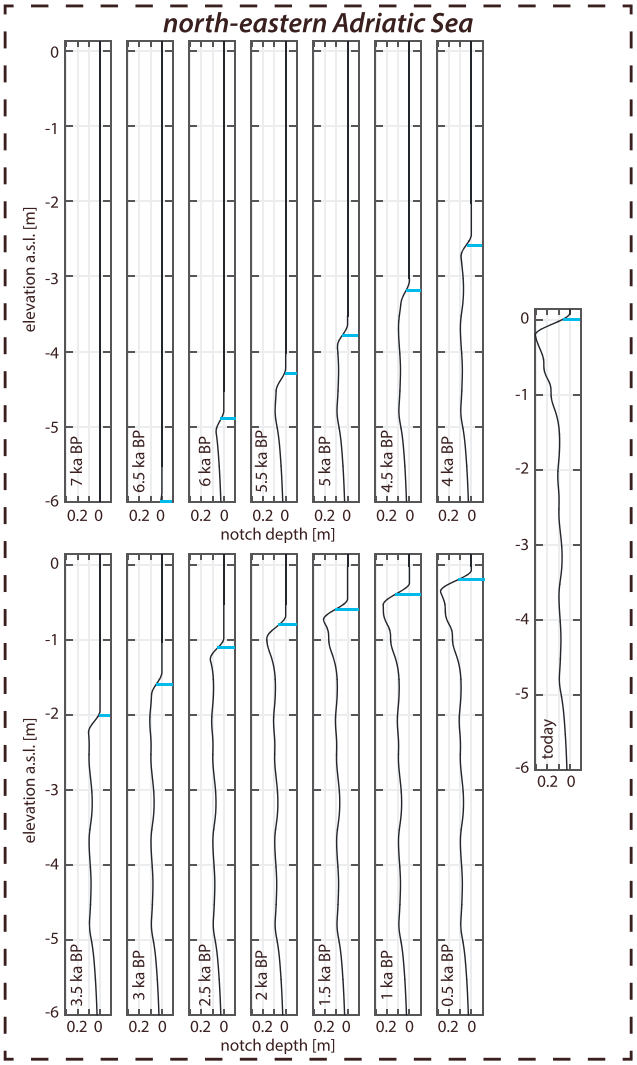

Figure 11. Modeled time slices of notch sequence development in subsiding regions. The blue lines indicate sea level at that time.

the cliff began ~6.7 kyr B.P. Approximately 1000 years later the rate of sea level change lowers again and causes deeper grazing up to ~0.1 m. However, ~2.9 kyr B.P. a distinct notch begins to form, at around −0.8 m. Subsequent lowering the rate sea level rise causes enhanced penetration per level while still distinct widening can be observed. A distinct notch is finally formed at ~0.7 kyr B.P. with the inflection point just below present-day sea level (Figure 10).

The sea level at Carmel Coast (Israel) has risen by not more than ~4 m since ~6.8 kyr B.P., with only ~0.5 m increase during the last 2800 years. This means that from 6.8 to 2.8 kyr B.P. sea level rises in average at ~0.9 mm/yr, and afterward at ~0.2 mm/yr. The latter rate coincides with uplift rates estimates by *Sivan et al.* [2001] (Figure 6f), which is why notch formation is expected to occur during the latest times of the Holocene, and furthermore not higher than at present datum. However, the results in Figure 10 show that the potential of considerable erosion is already given 5.8 kyr B.P. The erosional base evenly rises until ~3.9 kyr B.P. and causes a 1 m wide band along the vertical cliff with an average period of water contact of ~300 years; the resulting depth is ~0.15 m. A subsequent period of ~1100 years prolongates the contact time to ~400 years due to a lowered rate of sea level rise. At an erosion rate of 0.5 mm/yr the cliff gets deepened by 0.2 m during that period (Figure 10b). Since the given tidal range of 0.3 m already extends to the corresponding datum at that time, the floor of the most recent notch develops. A complete overlap of both rates, sea level rise and net uplift, occurs for the last 900 years resulting in a notch of >1 m depth at present-day sea level.

It is obvious that both regions experience similar evolution of tidal notch development. For both regions the same net uplift values are applied. The differently shaped sea level curves determine the calculated depth and significance of modeled notches. However, overall evolution and resulting cliff morphology bear resemblance at both parts of the Mediterranean.

5.4. Subsiding Coasts: NE Adriatic Sea

Coastal subsidence (−0.35 mm/yr [*Lambeck et al.*, 2004]) causes steeper gradients within the evolution of erosional levels than coastal uplift (Figure 6g). The trend-corrected sea level curve for the NE Adriatic has average rates of ~1.2 mm/yr from 6 to 2.7 kyr B.P. and ~0.4 mm/yr since 2.7 kyr. Therefore, indentations are expected to be not as deep as in uplifting regions. Modeled time slices in Figure 11 reveal that erosion begins ~6 kyr B.P. carving the cliff down by ~0.1 m. This means, already by that time, that the erosional zone affects the same cliff section for ~200 years at a modeled erosion rate of 0.5 mm/yr. Except for a few minor vertical

undulations the resulting cliff is carved by the same rate for the subsequent 3300 years. At approximately 2.7 kyr B.P. the lowered gradient of erosional base migration causes deeper incision at > -1 m asl on the modern cliff (Figure 11). The erosion rate exceeds the absolute vertical motion value which results in predominant notching rather than widening of the indentation. However, the recently developing notch at ~ -0.2 m asl is 0.3 m deep and is the result of a gradual uplift shift of the erosive tidal zone.

5.5. Introducing Cliff Slope and Coseismic Activity to the Model

Pirazzoli [1986] already pointed out the influence of sloping cliff faces. In particular, cliffs dipping gentler than 90° require more time to develop distinct notch morphologies, and the resulting notch shape will be asymmetrical with short roofs and long floors. However, this is the result of cumulative erosion over several years. The erosional potential remains normally distributed within the tidal range, which is why only the dip of the cliff face has to be adjusted in the model input. Here a moderate-high angle cliff slope of 80° is chosen causing asymmetrical notch shapes while preserving the ability to form distinct features.

A famous cliff face exhibiting tidal notch morphologies that are repeatedly associated with coseismic events is located at the north-western tip of Perachora Peninsula in the Alkyonides Gulf [e.g., *Kershaw and Guo*, 2001; *Pirazzoli and Evelpidou*, 2013]. *Pirazzoli et al.* [1994] identified four shorelines each offset by ~0.8 ± 0.3 m with estimated recurrence intervals of 1600 years from dating organic material of three notches at Heraion (Table 2). The strandline that was not dated (+1.7 m asl) by the authors is here calculated in accordance to the estimated recurrence interval and average displacement.

Introducing coseismic uplift events creates a stepwise modification to the emerging coast function in our model (Figure 12a). Dependent on the rate of relative sea level change the adjustments to the function representing coastal movements cause a prolongation of notch formation or result in the development of a new notch generation. Considerable erosion begins ~6.6 kyr B.P. and thus forms no difference to the model without coseismic uplifting events. However, a much higher position (~ +0.6 m) on the modern cliff face than without a correction for relative vertical land movements (~ −2.4 m; see Figure 7b) is obvious. A significant shift occurs until ~5 kyr B.P. ending up in notch formation at ~ +2.5 m (asl) prior to coseismic event 1. The first event lowers the erosional base by 0.6 m. As a consequence the former strandline is lifted above the tidal range and a new notch generation develops at ~ +2.2 m (asl). At that time (~4.4–2.4 kyr B.P.) the rate of sea level rise is still significantly different from the applied uplift rate causing upward carving and erosion of preexisting erosional features. Prior to event 2 the erosional base is located at ~ +2.8 m (asl) forming a second notch generation during relative stagnation of ~300 years. The accompanying 0.9 m coseismic uplift of event 2 throws the erosive zone back to a corresponding level at ~ +2.0 m. As the modeled scenario without coseismic uplift events already showed (see Figure 7b) the last ~2000 years are dominated by stagnation of the erosional base. Thus, in periods between events 2 and 3, and between events 3 and 4 distinct notches form at ~ +2.0 m and ~ +1.3 m (asl). The sloping cliff morphology causes an asymmetrical appearance of both notch generations as predicted by *Pirazzoli* [1986]. Subsequently, event 4 displaces the preexisting prominent strandline and results in the development of a new notch generation at modern sea level. The projection of the erosional base on the modern cliff face shows slight shifting prior to ~2.5 kyr B.P. As a result, vertical carving instead of horizontal deepening is the dominant erosive factor. Excluding the recently developing tidal notch, the cliff face exhibits three to four distinct indentations whose individual position on a modern cliff are further associated with coseismic events.

A second scenario including coseismic uplift events is modeled for the western Gulf of Corinth. Estimates on coseismic footwall uplift values per event and dated shorelines from *Stewart and Vita-Finzi* [1996] serve as input parameter additional to those already introduced in section 5.1. The authors dated two raised shorelines (1.8 m and 3.7 m asl) along the Eliki Fault to 1680 ± 130 yr B.P. for the lower strandline and 2290 ± 115 yr B.P. and 2600 ± 265 yr B.P. for the upper notch. Furthermore, they found no expression which can be attributed to a surface rupturing event that happened 1861 A.D. However, from these dates an earthquake recurrence interval of ~700 years is assumed here. Earthquake events of *M*6.0–7.0 as found from normal faulting events elsewhere tend to produce coseismic footwall uplifts of 0.2–0.3 m [e.g., *Jackson et al.*, 1982; *Papanikolaou et al.*, 2010]. Therefore, the scenario includes 11 earthquakes accompanied by normal distributed coseismic uplifts ranging from 0.2 to 0.3 m within a period of ~8000 years (Table 2). Events 1 and 2 produced surface displacements during periods of unstable sea level conditions. Therefore, no offset erosional expressions result from these two events. The first notch begins to form ~6.7 kyr B.P. at ~ +3.6 m

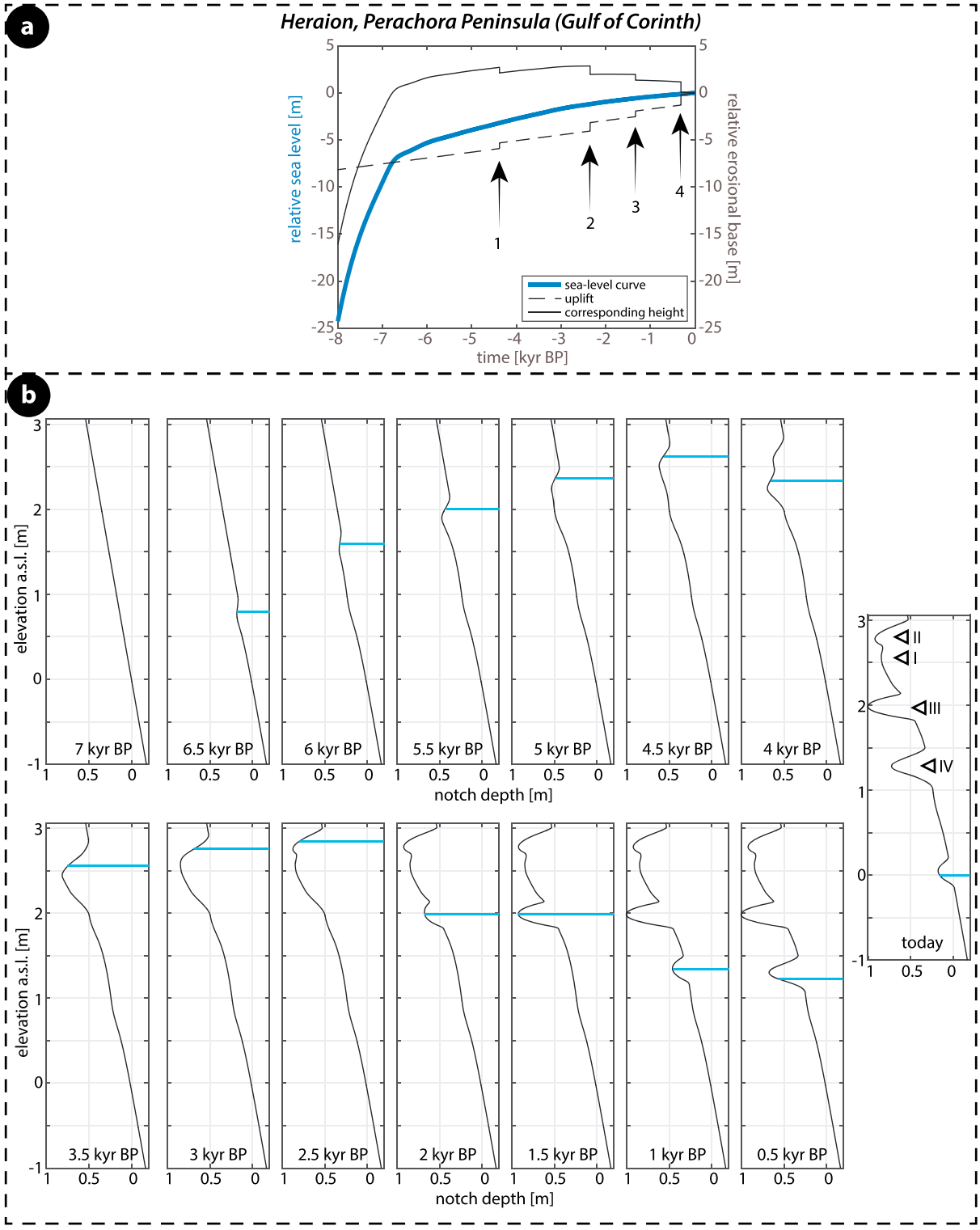

Figure 12. Results for the Heraion site in the eastern Gulf of Corinth including coseismic activity. (a) Coseismically modified progression of the erosional base. The arrows refer to events listed in Table 2. (b) Modeled notch sequence evolution including coseismic uplifting events dated by or inferred from *Pirazzoli et al.* [1994]. The triangles indicate erosional features at corresponding mean sea level on the modern cliff in between two coseismic uplift events. The blue lines indicate sea level at that time.

but widens up to a level of ~ +4.1 m because of minor sea level changes outpacing the coastal uplift. Event 3 lowers the erosional base to a corresponding height of ~3.9 m. The subsequent 700 year period is dominated by stagnation of the relative erosional base forming a distinct notch of ~0.3 m depth (Figure 13b, IV). The ensuing period of ~1400 years contains two events (4 and 5) that stepwise lower the relative erosional base which stays at a gradient of almost zero apart from that. The resulting notches (V and VI) comprise erosional contributions from 3000 years before. A distinct notch (VII) forms from ~3.8 to 3.0 kyr B.P. without noteworthy vertical shifting. During the period between event 7 and 8 notch VIII develops at ~ +2.8 m but gets widened due to a small component of gradual lowering the relative erosional base. The same process happens to notch IX that develops at ~2.0 kyr B.P. Even more obvious is the widening effect for the last two notches (X and XI), which are still separated from each other due to the successive uplifts from events 9 and 10. However, a sea level rise slower than modeled uplift causes a gradual lowering of the relative erosional base in the latest Holocene period. The predicted modern cliff morphology shows nine different historical sea levels ranging from ~ +0.7 m to +4.0 m. While uppermost notch generations (III–VI) appear stacked and concentrated, younger notch generations (IX–XI) are more spread along the vertical cliff. Presumably, the uppermost notch generations (III–VI) would not be differentiable in the field since their vertical spread is only 0.5 m and thus just exceeds the applied tidal range.

6. Discussion

The focus of this study has been to visualize tidal notch formation during the late Holocene, incorporating sea level change, coastal uplift/subsidence, erosion rates, coseismic activity, and cliff steepness. We have been able to show how coastal cliff morphologies develop within a migrating tidal range [see also *Pirazzoli*, 1986; *Evelpidou et al.*, 2011a, 2011b; *Trenhaile*, 2016] using actual late-Holocene sea level curves for the Mediterranean. The tidal range shifts along a vertical cliff due to gradual relative sea level changes optionally accompanied by coastal tectonic activity. In the following discussion, the contributions of slow and rapid vertical shifts of the erosional base are discussed with regards to the applied modeling parameters.

6.1. Modeling Parameters and Inputs

The modeling algorithm we present here deals with ideal conditions. Therefore, the results do not represent actual and naturally existing cliff faces.

First, these ideal conditions incorporate a perfectly sheltered site, where tidal range is low and constant [*Pirazzoli*, 1986]. Assuming the absence of spray enables us to ignore notch roof modification by haloclastic processes above the high tide level. In addition, carbonate lithologies sheltered from strong wave action enable grazing or coring organisms to settle and contribute to the erosion in vegetational bands within the midlittoral zone [*Torunski*, 1979]. Moreover, *Pirazzoli* [1986] points out that only in sheltered sites does the midlittoral zone equal the tidal range. Since the model calculates erosive effects only for the applied tidal range of 0.3 m [*Evelpidou et al.*, 2012b; *Evelpidou and Pirazzoli*, 2016], predicted profiles correspond to natural sites without strong wave action. If a different tidal range is used, then the affected parts of the cliff vary accordingly. Hence, a smaller tidal range yields narrower indentations whereas a wider tidal range increases width of a tidal notch [see also *Trenhaile*, 2014]. When the erosional base varies through time narrow notches appear to have greater separation than wider features.

Second, the algorithm was designed to model tidal notches formed within the tidal range without significant contributions by wave quarrying, sediment abrasion, or chemical weathering. Mechanical wave erosion is of a second order when unbroken waves are reflected from steep cliffs and when a source for abrasive material is absent. Moreover, wave quarrying is most common in storm wave regions and where coastal cliffs are composed of rocks with structural discontinuities [*Trenhaile*, 2015]. The majority of carbonate coastlines throughout the Mediterranean do not have plunging cliffs and/or are located next to beaches, or are fronted by wave breaking foreshores. However, steep cliff faces of massive limestones located far from abrasion material such as sands and pebbles exist. Indeed, carbonate cliffs tend to develop karst formations which may be accompanied by freshwater exchange. If so, the seawater is locally diluted, and thus, chemical dissolution of calcium carbonate contributes little to the overall erosion rate. Moreover, the solubility of calcium carbonate is higher at low temperatures. This leads to the assumption that during the glacial period lower water temperatures in general and higher precipitation resulted in higher amounts of limestone dissolution. However, *Evelpidou et al.* [2011b] suggest using the term "visor" for notch profiles where the base is missing

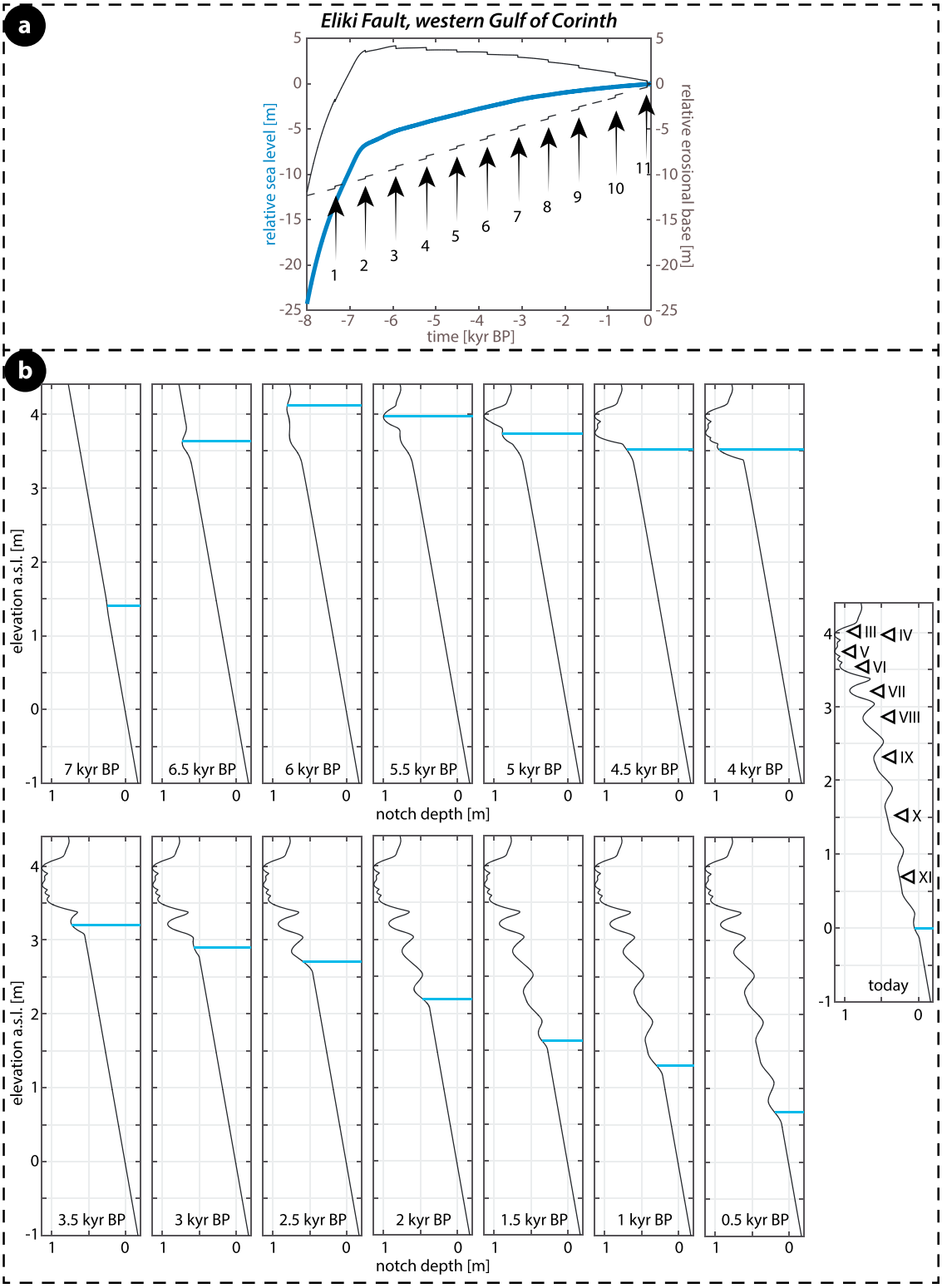

Figure 13. Results for the Eliki site in the western Gulf of Corinth including the coseismic activity of 11 events. (a) The local sea level curve and landmass evolution exhibiting coseismic uplifts. (b) Modeled time slices of cliff face evolution. The triangles indicate erosional features at corresponding mean sea level on the modern cliff in between two coseismic uplift events. The blue lines indicate sea level at that time.

due to chemical dissolution. For such localized phenomena notch developing effective erosion is not limited to the tidal range, and hence, those morphologies are not suitable sea level markers. Herein, model predictions aim to illustrate the evolution of paleostrandline sequences as they are commonly used to infer coastal coseismic activity [e.g., *Pirazzoli et al.*, 1982, 1989, 1991, 1994; *Stewart and Vita-Finzi*, 1996; *Kershaw and Guo*, 2001]. Furthermore, late Holocene tidal notches develop in the hot and semiarid environment of the Mediterranean. This circumstance decreases the ability of limestone dissolution, in general.

Third, vertical lithological inhomogeneities are not considered. Varying bedrock consistency and accompanying erosion rates are not modeled. Consequently, the profiles represent homogeneous limestone cliff morphologies resulting from even erosion at 0.5 mm/yr [e.g., *Evelpidou et al.*, 2012b; *Furlani and Cucchi*, 2013, *Pirazzoli and Evelpidou*, 2013]. Dating tidal notches and deriving erosion rates is a challenging task since radiocarbon-bearing dating material is of very sensitive organisms that can easily be eroded by various agents after their displacement [e.g., *Evelpidou and Pirazzoli*, 2016]. However, some efforts have been undertaken to derive estimates for erosion rates across the Mediterranean. The applied erosion rate is in good correlation with recently derived estimates from a well-dated fossil tidal notch in Greece (0.64 mm/yr) [*Evelpidou and Pirazzoli*, 2016] and from microerosion meter measurements in the northern Adriatic (0.31 mm/yr) [*Furlani and Cucchi*, 2013]. In general, it should be noted that varying the applied erosion rate in different model runs modifies the predicted indentation depth but not its position [see also *Trenhaile*, 2014].

Fourth, modeled notches are not constructed to collapse. Overburden that cannot be supported by the lithology results in cliff collapse, which is basically controlled by the depth of a notch. *Trenhaile* [2014] includes the ability of cliff collapse in his modeling approach and concludes that failure is mainly dependent on the maximum notch depth. For collapse scenarios the author used maximum notch depths of 2 m. However, the notch profiles predicted herein do not exceed 1.5 m in depth (see Figure 7a). Moreover, if cliff collapse occurs environmental conditions change likely resulting in significantly different wave action and constitute a possible sediment origin [*Trenhaile*, 2015]. This would clearly contradict other model assumptions at a certain point.

Fifthly, horizontal differences are not displayed by a two-dimensional notch profile. Fault movement leading to differential uplift, local variations of wave and surf regimes, and horizontal bedrock heterogeneity are reasons for differing notch profiles on a local scale [e.g., *Kershaw and Guo*, 2001].

The five listed caveats imply significant simplifications to the model. Each of above mentioned points has considerable influence on the shape of a notch profile. Furthermore, the combination of all of them is considered to modify a tidal notch for each investigated region individually. However, considering such assumptions enables the development of a mathematical model of a symmetrically effecting erosion potential within the tidal range per year. Then, cumulative erosion depicts the base for the static notch developing model that only distinguishes between continuous erosion per level or not.

Predicting actual scenarios using local sea level curves and regional landmass movements is a novelty to the assessment of tidal notches as earthquake geological effects. Conceptual models [e.g., *Pirazzoli*, 1986; *Evelpidou et al.*, 2011a, 2011b] indicate shape modification by sea level change and even already distinguish slow and rapid changes of the erosional base. *Trenhaile* [2016] modeled notch formation considering linear and sudden sea level changes as well. In contrast to the model presented in here, the author also considers changing erosional efficacy, cliff collapse [see also *Trenhaile*, 2014], and varying rock resistance. However, by simplifying the model assumptions and orienting to specific regions we were able to achieve similar conclusions regarding the influence of local- and regional-scale factors and to confirm that. Similar profiles can be produced by different combinations of incorporating factors [see *Trenhaile*, 2016]. One difference between Trenhailes's and our models is the applied distribution of the erosional potential. Where *Trenhaile* [2016] uses a linear function we consider a distribution following a quadric polynomial based on repeated immersion of cliff parts due to tides following a sine function in a long-term average (Figure 4). Erosion rates measured at different heights (vertical resolution is 0.25 m) over a 3 year period on a limestone slab in the northern Adriatic indicate that the mean downwearing rate follows a symmetrical shape [*Furlani and Cucchi*, 2013]. Long-term measurements will show what is the best fit function describing the erosional potential distribution. However, since both models yield similar results the fitting appears to be of a second order. As a major difference between both models *Trenhaile* [2016] constructed a more theoretical approach, while we clearly orient at region-specific conditions. Hence, our model provides the opportunity to compare natural

occurrences of tidal notch sequences with derived scenario interpretations. Existing investigations and interpretations on coseismic tectonic history might have to be reassessed due to so far unknown consequences concerning submerged notches and/or timing and magnitude of coastal coseismic activity.

Therefore, the most dynamic component in the model is the applied sea level curve. The shape, rates, punctual characteristics, and the overall richness of details of a sea level curve form fundamental input for the dynamic model (Figures 6 and 10). Commonly, a variety of sea level indicators are used to reconstruct sea level history. Typically, these indicators are of biological, sedimentological, erosional, and archaeological remnants [*Lambeck et al.*, 2004; *Kelletat*, 2005a]. However, the spatial distribution across the Mediterranean, concentration of certain markers in some places, and differential tectonic activity cause gaps in the availability of local sea level curves (e.g., Spain and North Africa) [*Pirazzoli*, 1991] and vary the quality. By contrast, many sea level curves have been published for shores at southern France, the Aegean, the Levant, and the Adriatic in the past decades. All histories applied here have a significantly changing rate of sea level rise plotted in the period between 7 and 6 kyr B.P. A global meltwater pulse caused rapidly changing sea levels (10–20 mm/yr) until 7 kyr B.P. (Figure 5a), before slow-moderate (0.2–2 mm/yr) rise adjusts in the mid-Holocene. *Lambeck et al.* [2014] point out that in the past 6.7 kyr B.P. only 4 m of global sea level rise took place, which equals an average rate of ~0.6 mm/yr. Moreover, the authors predict actually two stages of sea level rise, the first going from 6.7 to 4.2 kyr B.P. and the second covering the last Holocene period. Following their estimates, 75% of mid-Holocene sea level rise took place during the first stage (1.2 mm/yr). Sea level changing at ~0.2 mm/yr during the second stage is broadly consistent with other studies [e.g., *Pirazzoli*, 1991]. For the Mediterranean Sea a third trend of 1.7 mm/yr covering the past century is predicted by *Wöppelmann and Marcos* [2012]. However, the last is not considered in this study since the applied erosion rate of 0.5 mm/yr produces indentation of 5 cm only in 100 years of relative stand-still. Furthermore, this high-rate change still does not submerge the cliff from the tidal range of 0.3–0.4 m [*Lambeck et al.*, 2004; *Evelpidou et al.*, 2012b; *Antonioli et al.*, 2015] within this short period. The local sea level curves applied to test the algorithm are consistent with overall characteristics described above. However, the relative sea level at the knickpoint around ~6.5 kyr B.P. varies as well as the timing for the second rate lowering period. While the relative sea level was ~6–7 m below present datum (Figures 6a–6d) in the central Mediterranean since the mid-Holocene, an ~3–4 m rise occurred in the eastern parts of the basin (Figures 6e, 6f, and 6h). The second, more minor change generally appears between 3 and 2 kyr B.P. and thus later as predicted from the global sea level curve [*Lambeck et al.*, 2014]. Furthermore, in the central basin this change tends to occur at ~3.0–2.5 kyr B.P. while the eastern Sea reaches this point ~500 years later [e.g., *Sivan et al.*, 2001].

6.2. Solving the Issue With Submerged Notches

In regions of significant tectonic activity reconstructing the sea level history is problematic since most sea level indicators refer to some specific part of the tidal range and their displacement by fault activity requires accurate adjustments to resultant vertical motion. *Roberts et al.* [2009] demonstrated the variability in uplift even over short distances along fault strike. Yet tectonic activity is essential for estimates of long-term landmass uplift/subsidence. Hence, for regions such as the seismically high-active Gulf of Corinth it is unlikely that representative estimates for both, sea level history and paleo-tectonic rates, will be found. In such cases assumptions and spatial generalizations have to be made; for instance, the sea level curve for the shore of Peloponnese is representative at least for the western part of the Corinthian Gulf.

Interestingly, *Boulton and Stewart* [2015] hypothesized that in order to initiate notch formation uplift rates needed to equal rates of sea level rise. This statement presumes that subsiding coasts will not experience a relative stagnation under conditions of steadily rising sea levels and that subsiding coasts are not suitable for tidal notch development without more complex tectonic movements involved during the late Holocene.

The difference between relative sea level and corresponding landmass position forms the relative erosional base projected on a modern cliff face. Different uplift rates applied to the same sea level curve have a huge impact on the shape of erosional base evolution (Figures 6a and 6b). As a result, tidal notches form at different periods and appear on different corresponding levels (Figures 7 and 14a). Furthermore, a combination of low coastal uplift rates (<1 mm/yr) and significant sea level change since the mid-Holocene yields tidal notches to appear below present-day sea level. Coasts that are considered to provide stable conditions potentially exhibit submarine notches (Figure 10). Here the model is confirmed by observations made at the southern Levantine coast by *Goodman-Tchernov and Katz* [2015]. The authors concluded that sea level

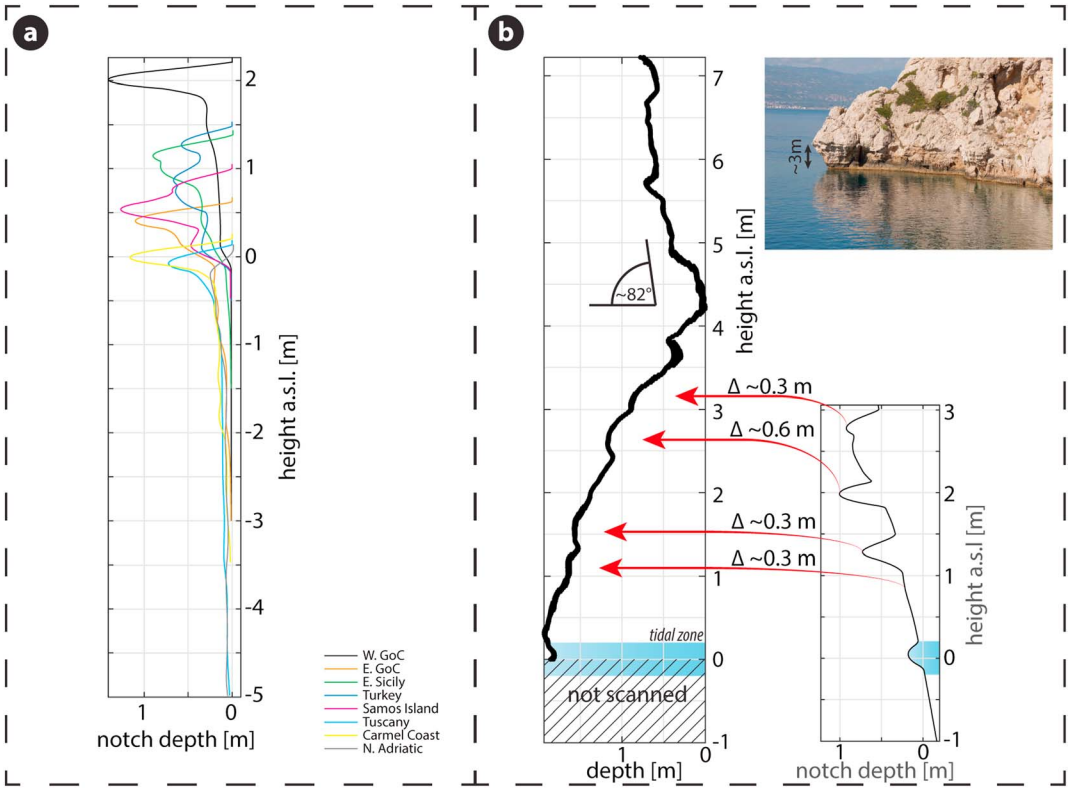

Figure 14. Comparing the model to reality. (a) Comparison of all modeled notch profiles free from coseismic displacements. (b) Comparison of modeled notch profile (E. Gulf of Corinth) containing coseismic uplifts to an actual notch profile extracted from TLS data at Cape Heraion, Perachora Peninsula [after *Schneiderwind et al.*, 2017].

history provides a period of relative stagnation, followed by drowning. At a coast that is generally considered to be not tectonically affected, only eustatic characteristics provide potential for notch development.

The results modeled from subsiding coastal conditions show that relative stagnation does not mean sea level rise and vertical landmass motion have to occur in unison. In detail, modeled cliffs get significantly carved when the erosional base shifts at $<$1.1 mm/yr using an overall erosion rate of 0.5 mm/yr [see also *Trenhaile*, 2016]. Moreover, horizontal deepening dominates vertical carving when the difference between vertical land motion and sea level rise is $<$0.5 mm/yr. This implies that a notch in a limestone cliff (erosion rate: 0.5 mm/yr) that develops while sea level rise or landmass motion dominates by 0.5 mm/yr for about 200 years is ~0.1 m deep and ~0.4 m high (including 0.3 m tidal range). When introducing the effect of varying tides, spray, and weathering the interpretation of such an expression would most likely conclude a "relative stagnation" to form it. Even the occurrence of a notch located on a subsiding coast becomes plausible if vertical relative land motion does not exceed the absolute threshold value. *Benac et al.* [2004] described submerged notches in the northern Adriatic. Their results show well expressed but asymmetric tidal notches always submerged by at least 0.2 m indented between 0.18 and 1.50 m. These values range in the same order as our modeled notch estimates.

6.3. The Role of Coseismic Displacements

The modeled cliff sections show the significant impact of the sea level curve shape on time and duration of notch formation in accordance to a given constant coastal uplift/subsidence. Dependent on the shape of the sea level curve the cliff morphology results from grazing, incising, and overwriting only from gradual climatically driven sea level changes. When introducing coseismic activity to the model even more dynamics are addressed in the system. The abrupt migration of the erosional base potentially yields to the development of an entirely new notch generation. However, in combination with an arcuate-shaped erosional base height curve (Figure 6) the migration is not oriented purely in one direction. Furthermore, repeated coseismic

activity results not necessarily of the same migration stepsize since rates of a mean relative sea level change vary from ascending (~6 kyr B.P.) to flat (~4 kyr B.P.), and also descending (~2 kyr B.P.). As a result, lower sections of a modern cliff face potentially formed the strandline at least two times since 7 kyr B.P. (Figures 6a–6c and 12a).

In particular, modeled results for the southern Italian coastline show how repeated erosion modifies the developing cliff face (Figure 8). When introducing coseismic displacements to the model, modification is even more apparent. Both scenarios where coseismic uplift was included indicate that coseismic offset possibly results in one of two options: (i) rapid displacement of the erosional zone causing the development of an entirely new notch generation, which likely overprints older features to a greater or lesser degree (Figure 13a), or (ii) prolonging or re-entering the erosive phase at a certain level in periods of gradual sea level change (Figure 12a). Furthermore, the scenario modeled for Heraion illustrates that a notch sequence on a modern cliff from top descending to sea level is not inevitably of decreasing age caused by coseismic uplift events in periods of slightly uplift outpacing sea level rise. Moreover, when rapid coseismically induced displacement prolongs the erosive phase the modern expression cannot be used to infer information about the specific event since it only causes deepening of the preexisting notch.

6.4. Model Versus Reality

The reliability of both scenarios modeled for the western and eastern parts of the Gulf of Corinth should not be overvalued due to idealized assumptions and generalizations according the applied sea level curve. The two different scenarios of seismological history are applied since they pose results from different views. The inputs for the Heraion model are inferred from a study that aimed to directly investigate episodic uplift deduced from Holocene shorelines [*Pirazzoli et al.*, 1994]. The differences between model and natural cliff are most likely the result of the inherent model assumptions, a sea level curve not specifically estimated for that region, and onshore tectonic activities which are not considered in the model (Figure 14b). However, modeled tidal notches and minor indentation can be correlated to actual observations. For instance, notches modeled to +1.4 m and +2.8 m might coincide with observed expressions at +1.7 m and +3.1 m. Even depth relations between modeled and natural notches resemble each other in appearance. On the natural cliff the notch at +2.6 m forms the deepest indentation of the natural sequence which matches with the notch modeled to +2.0 m. In fact, no significant indentation is modeled in between these notches giving evidence for cumulative offsetting contributed by both coseismic uplift and gradual relative sea level change. However, balancing smaller coseismic uplift values from offshore origin and down-throwing contributions from active on-shore faults potentially result in more paleo-strandlines than observed so far [*Schneiderwind et al.*, 2017].

The Eliki Fault scenario is based on the assumption of a regular seismic cycle with multiple coseismic uplift events each of 0.2–0.3 m [*Stewart and Vita-Finzi*, 1996]. Uplift values of this range and recurrence interval (not exceeding 1000 years) are plausible and consistent with paleoseimological principles in extensional tectonic settings [*Jackson et al.*, 1982; *Papanikolaou et al.*, 2010]. The results for this scenario are more consistent with reports of the natural cliff face. *Stewart and Vita-Finzi* [1996] described prominent notch levels at +1.8 m dating to 1680 ± 130 years B.P. and at +3.7 m dating to 2290 ± 115 years B.P. and 2600 ± 265 years B.P. Varying dating results for the upper notch might be the consequence of repeated erosive phases compressed along a thin section of the cliff. In the modeled cliff a tidal notch develops at +1.8 m as a consequence of coastal displacement at 1680 years B.P. and hence misses natural conformity only at one earthquake recurrence interval. The absence of a distinct erosive evidence for an earthquake that happened 1861 A.D. might be the consequence of an increasing amount of downward carving due to fluctuating gradients (relative sea level and coastal uplift).

Therefore, our model shows promise for the potential reconstruction of actual cliff faces but needs better and more accurate input values for relative sea level change and seismic history. However, in accordance with the assumptions made the algorithm combines the results from multiple disciplines and produces cliff faces that can be compared to natural exposures to support interpretation strategies. If the sea level rise is well constrained, far range deglaciational effects are validated, and information about paleotectonic activity is available, a separation of spatial and temporary segments might be possible. However, to produce more reliable results parameters such as maximum overburden, lithological discontinuities, exposure to wave action, and much more have to be considered [*Trenhaile*, 2014]. Furthermore, constraining the erosional base does not only include isostatic corrected sea levels but also tectonic activities on and offshore. In extensional

Graben systems such as the Gulf of Corinth several coast-down-throwing normal faults on land potentially influence the erosional level. This research has implications for assessing the overall and local seismic activity of a certain region. Based on reasonable assumptions reliable information on overall tectonic activity as a budget and balanced structure-linked values can be gathered. Due to its simplicity the novel algorithm is transparent and reproducible increasing the objectivity in assessing coast-affecting tectonic activity.

7. Conclusions

Depending on the region and associated local sea level history, Holocene tidal notches can form from 6000–7000 years B.P. in the Mediterranean Basin [see also *Trenhaile*, 2016]. Thereby, the very early stages of counterbalanced eustatic and isostatic conditions might not result in the most elevated sea level marker at the present day. In detail, modern cliff morphology contains indentations, nips, and deepened sections that are not true notches. This geomorphology is a product of continuous notch formation, repeated overprinting, bedrock heterogeneity, and storm surge elevations. Gradual sea level change optionally accompanied by tectonic activity shifts the erosional base along the vertical axis (see also Figure 3). As a consequence, a notch sequence from top descending to sea level does not necessarily adhere rigidly to and old-to-young chronology. Stages of almost-stagnation between regional sea level rise and coastal uplift tend to produce more space between individual notch generations. However, resulting notch shapes appear widened in comparison to successively older features.

The developed algorithm is not as close to reality as required for a retrodeformation due to significant generalizations and simplifications. However, the model presented is the first that incorporates actual and region-specific Holocene sea level changes, erosion rates, and landmass movements (slow and rapid). It points out how variable tidal notch development and preservation occurs even in local scale. Paleoseismological studies should benefit from its application since it provides a method for the evaluation of field observations and interpreted meanings. Case studies considering both coastal coseismic footwall uplift from offshore normal faults and coast downthrowing onshore faults could profit by evaluating the balance of relative motions.

Our conclusions are summarized as follows:

1. The algorithm makes clear how slow and rapid processes interplay and bias each other (modification).
2. The visualization illustrates how slow and gradual sea level changes can result in sequences that look similar to those generated with influence of seismic activity.
3. A notch offset exceeding several decimeters in a present-day notch sequence is not a contrariety to typical coseismic coastal footwall uplifts since recurrent overprinting and minor sea level variation can produce such offsets even without tectonic activity. Therefore, tidal notches may not be used as primary earthquake geological effects without considering detailed sea level history.
4. Submerged notches can occur on emerging coastlines.
5. "Relative stagnation" is not a condition with the absence of relative motion but comprises a scope of minor motion ($<$0.5 mm/yr) in dependency of the actual penetration period and erosion rate.

The model presented enables researchers to have an enhanced understanding of the evolution of tidal notch sequences and points out how important reliable data of sea level rise and coastal uplift are to the correct interpretation of such sequences.

Acknowledgments

T.M. Fernández-Steeger (RWTH Aachen University) is acknowledged for financial support and fruitful discussions. We thank the Editor Giovanni Coco and the Associate Editor Curt Storlazzi as well as Alan S. Trenhaile and an anonymous reviewer for their comments and suggestions, which significantly improved our manuscript. The data used are listed in the references. Supporting data are included as 10 video files in a supporting information file; any additional data may be obtained from S. Schneiderwind (e-mail: s.schneiderwind@nug.rwth-aachen.de). Tide gauge data for Figure 4 a has been provided by the Hellenic Navy Hydrographic Service (HNHS). We note that there are no data sharing issues since all of the numerical information is provided in the figures produced by solving the equations in the paper.

References

Antonioli, F., L. Ferranti, K. Lambeck, S. Kershaw, V. Verrubbi, and G. Dai Pra (2006), Late Pleistocene to Holocene record of changing uplift rates in southern Calabria and northeastern Sicily (southern Italy, Central Mediterranean Sea), *Tectonophysics*, *422*(1–4), 23–40, doi:10.1016/j.tecto.2006.05.003.

Antonioli, F., et al. (2015), Tidal notches in Mediterranean Sea: A comprehensive analysis, *Quat. Sci. Rev.*, *119*, 66–84, doi:10.1016/j.quascirev.2015.03.016.

Armijo, R., B. Meyer, G. C. P. King, A. Rigo, and D. Papanastassiou (1996), Quaternary evolution of the Corinth rift and its implications for the late Cenozoic evolution of the Aegean, *Geophys. J. Int.*, *126*(1), 11–53, doi:10.1111/j.1365-246X.1996.tb05264.x.

Ayat, B. (2013), Wave power atlas of eastern Mediterranean and Aegean Seas, *Energy*, *54*, 251–262, doi:10.1016/j.energy.2013.02.060.

Benac, Č., M. Juračić, and T. Bakran-Petricioli (2004), Submerged tidal notches in the Rijeka Bay NE Adriatic Sea: Indicators of relative sea-level change and of recent tectonic movements, *Mar. Geol.*, *212*(1–4), 21–33, doi:10.1016/j.margeo.2004.09.002.

Besio, G., L. Mentaschi, and A. Mazzino (2016), Wave energy resource assessment in the Mediterranean Sea on the basis of a 35-year hindcast, *Energy*, *94*, 50–63, doi:10.1016/j.energy.2015.10.044.

Boulton, S. J., and I. S. Stewart (2015), Holocene coastal notches in the Mediterranean region: Indicators of palaeoseismic clustering?, *Geomorphology*, *237*, 29–37, doi:10.1016/j.geomorph.2013.11.012.

Carcaillet, J., J. L. Mugnier, R. Koçi, and F. Jouanne (2009), Uplift and active tectonics of southern Albania inferred from incision of alluvial terraces, *Quat. Res.*, *71*(3), 465–476, doi:10.1016/j.yqres.2009.01.002.

Carminati, E., C. Doglioni, and D. Scrocca (2003), Apennines subduction-related subsidence of Venice (Italy). *Geophys. Res. Lett.*, *30*(13), 1717, doi:10.1029/2003GL017001.

Collier, R. E. L., M. R. Leeder, P. J. Rowe, and T. C. Atkinson (1992), Rates of tectonic uplift in the Corinth and Megara basins, central Greece, *Tectonics*, *11*(6), 1159–1167, doi:10.1029/92TC01565.

Cooper, F. J., G. P. Roberts, and C. J. Underwood (2007), A comparison of 10 3–10 5 year uplift rates on the South Alkyonides Fault, central Greece: Holocene climate stability and the formation of coastal notches, *Geophys. Res. Lett.*, *34*, L14310, doi:10.1029/2007GL030673.

Cundy, A. B., K. Gaki-Papanastassiou, D. Papanastassiou, H. Maroukian, M. R. Frogley, and T. Cane (2010), Geological and geomorphological evidence of recent coastal uplift along a major Hellenic normal fault system (the Kamena Vourla fault zone, NW Evoikos Gulf, Greece), *Mar. Geol.*, *271*(1–2), 156–164, doi:10.1016/j.margeo.2010.02.009.

Evelpidou, N., and P. A. Pirazzoli (2016), Estimation of the intertidal bioerosion rate from a well-dated fossil tidal notch in Greece, *Mar. Geol.*, *380*, 191–195, doi:10.1016/j.margeo.2016.04.017.

Evelpidou, N., P. A. Pirazzoli, A. Vassilopoulos, and A. Tomasin (2011a), Holocene submerged shorelines on Theologos area (Greece), *Z. Geomorphol.*, *55*(1), 31–44, doi:10.1127/0372-8854/2011/0055-0032.

Evelpidou, N., P. A. Pirazzoli, J.-F. Saliège, and A. Vassilopoulos (2011b), Submerged notches and doline sediments as evidence for Holocene subsidence, *Cont. Shelf Res.*, *31*(12), 1273–1281, doi:10.1016/j.csr.2011.05.002.

Evelpidou, N., A. Vassilopoulos, and P. A. Pirazzoli (2012a), Submerged notches on the coast of Skyros Island (Greece) as evidence for Holocene subsidence, *Geomorphology*, *141-142*, 81–87, doi:10.1016/j.geomorph.2011.12.025.

Evelpidou, N., I. Kampolis, P. A. Pirazzoli, and A. Vassilopoulos (2012b), Global sea-level rise and the disappearance of tidal notches, *Global Planet. Chang.*, *92-93*, 248–256, doi:10.1016/j.gloplacha.2012.05.013.

Evelpidou, N., P. A. Pirazzoli, and G. Spada (2015), Origin and Holocene evolution of a slightly submerged tidal notch in the NE Adriatic, *J. Coast. Res.*, *300*, 255–264, doi:10.2112/JCOASTRES-D-14-00016.1.

Faccenna, C., et al. (2014), Mantle dynamics in the Mediterranean, *Rev. Geophys.*, *52*, 283–332, doi:10.1002/2013RG000444.

Ferranti, L., C. Monaco, F. Antonioli, L. Maschio, S. Kershaw, and V. Verrubbi (2007), The contribution of regional uplift and coseismic slip to the vertical crustal motion in the Messina Straits, southern Italy: Evidence from raised late Holocene shorelines, *J. Geophys. Res.*, *112*, B06401, doi:10.1029/2006JB004473.

Furlani, S., and F. Cucchi (2013), Downwearing rates of vertical limestone surfaces in the intertidal zone (Gulf of Trieste, Italy), *Mar. Geol.*, *343*, 92–98, doi:10.1016/j.margeo.2013.06.005.

Furlani, S., F. Cucchi, S. Biolchi, and R. Odorico (2011), Notches in the northern Adriatic Sea. Genesis and development, *Quat. Int.*, *232*(1–2), 158–168, doi:10.1016/j.quaint.2010.06.010.

Goodman-Tchernov, B., and O. Katz (2015), Holocene-era submerged notches along the southern Levantine coastline: Punctuated sea level rise?, *Quat. Int.*, doi:10.1016/j.quaint.2015.10.107.

Grützner, C., S. Schneiderwind, I. Papanikolaou, G. Deligiannakis, A. Pallikarakis, and K. Reicherter (2016), New constraints on extensional tectonics and seismic hazard in northern Attica, Greece. The case of the Milesi fault, *Geophys. J. Int.*, *204*(1), 180–199, doi:10.1093/gji/ggv443.

Harrison, R. W., E. Tsiolakis, B. D. Stone, A. Lord, J. P. McGeehin, S. A. Mahan, and P. Chirico (2013), Late Pleistocene and Holocene uplift history of Cyprus: Implications for active tectonics along the southern margin of the Anatolian microplate, *Geol. Soc. London, Spec. Publ.*, *372*(1), 561–584, doi:10.1144/SP372.3.

Hollenstein, C., M. D. Müller, A. Geiger, and H.-G. Kahle (2008), Crustal motion and deformation in Greece from a decade of GPS measurements, 1993–2003, *Tectonophysics*, *449*(1–4), 17–40.

Jackson, J. A., J. Gagnepain, G. Houseman, G. C. P. King, P. Papadimitriou, C. Soufleris, and J. Virieux (1982), Seismicity, normal faulting, and the geomorphological development of the Gulf of Corinth (Greece): The Corinth earthquakes of February and March 1981, *Earth Planet. Sci. Lett.*, *57*(2), 377–397, doi:10.1016/0012-821X(82)90158-3.

Kelletat, D. H. (2005a), A Holocene sea level curve for the eastern Mediterranean from multiple indicators, *Z. Geomorph. N.F.*, *137*, 1–9.

Kelletat, D. H. (2005b), Notches, in *Encyclopedia of Coastal Science*, edited by M. L. Schwartz, pp. 728–729, Springer, Dordrecht.

Kershaw, S., and L. Guo (2001), Marine notches in coastal cliffs: Indicators of relative sea-level change, Perachora Peninsula, central Greece, *Mar. Geol.*, *179*(3–4), 213–228, doi:10.1016/S0025-3227(01)00218-3.

Koukouvelas, I., A. Mpresiakas, E. Sokos, and T. Doutsos (1996), The tectonic setting and earthquake ground hazards of the 1993 Pyrgos earthquake, Peloponnese, Greece, *J. Geol. Soc.*, *153*(1), 39–49, doi:10.1144/gsjgs.153.1.0039.

Laborel, J., C. Morhange, J. Collina-Girard, and F. Laborel-Deguen (1999), Littoral bioerosion, a tool for the study of sea level variations during the Holocene, *Bull. Geol. Soc. Den.*, *45*, 164–168.

Lambeck, K. (1995), Late Pleistocene and Holocene sea-level change in Greece and southwestern Turkey: A separation of eustatic, isostatic and tectonic contributions, *Geophys. J. Int.*, *122*(3), 1022–1044.

Lambeck, K., and A. Purcell (2005), Sea-level change in the Mediterranean Sea since the LGM: Model predictions for tectonically stable areas, *Quat. Sci. Rev.*, *24*(18–19), 1969–1988, doi:10.1016/j.quascirev.2004.06.025.

Lambeck, K., F. Antonioli, A. Purcell, and S. Silenzi (2004), Sea-level change along the Italian coast for the past 10,000 yr, *Quat. Sci. Rev.*, *23*(14–15), 1567–1598, doi:10.1016/j.quascirev.2004.02.009.

Lambeck, K., H. Rouby, A. Purcell, Y. Sun, and M. Sambridge (2014), Sea level and global ice volumes from the Last Glacial Maximum to the Holocene, *Proc. Natl. Acad. Sci. U.S.A.*, *111*(43), 15,296–15,303, doi:10.1073/pnas.1411762111.

Larson, M. P., T. Sunamura, L. Erikson, A. Bayram, and H. Hanson (2011), An analytical model to predict dune and cliff notching due to wave impact, *Int. Conf. Coastal. Eng.*, *1*(32), doi:10.9753/icce.v32.sediment.35.

Leeder, M. R., L. C. McNeill, R. E. Ll Collier, C. Portman, P. J. Rowe, J. E. Andrews, and R. L. Gawthorpe (2003), Corinth rift margin uplift: New evidence from late Quaternary marine shorelines, *Geophys. Res. Lett.*, *30*(12), 1611, doi:10.1029/2003GL017382.

Liberti, L., A. Carillo, and G. Sannino (2013), Wave energy resource assessment in the Mediterranean, the Italian perspective, *Renewable Energy*, *50*, 938–949, doi:10.1016/j.renene.2012.08.023.

De Martini, P. M., D. Pantosti, N. Palyvos, F. Lemeille, L. McNeill, and R. Collier (2004), Slip rates of the Aigion and Eliki faults from uplifted marine terraces, Corinth Gulf, Greece, *C. R. Geosci.*, *336*(4–5), 325–334, doi:10.1016/j.crte.2003.12.006.

McNeill, L. C., and R. E. L. Collier (2004), Uplift and slip rates of the eastern Eliki fault segment, Gulf of Corinth, Greece, inferred from Holocene and Pleistocene terraces, *J. Geol. Soc.*, *161*(1), 81–92, doi:10.1144/0016-764903-029.

McNeill, L. C., C. J. Cotterill, T. J. Henstock, J. M. Bull, A. Stefatos, R. E. L. Collier, G. Papatheoderou, G. Ferentinos, and S. E. Hicks (2005), Active faulting within the offshore western Gulf of Corinth, Greece: Implications for models of continental rift deformation, *Geology*, *33*(4), 241, doi:10.1130/G21127.1.

Papanikolaou, D., and I. Papanikolaou (2007), Geological, geomorphological and tectonic structure of NE Attica and seismic hazard implications for the northern edge of the Athens plain, *Bull. Geol. Soc. Greece*, *40*, 425–438.

Papanikolaou, D., and L. H. Royden (2007), Disruption of the Hellenic arc: Late Miocene extensional detachment faults and steep Pliocene-Quaternary normal faults—Or what happened at Corinth?, *Tectonics*, *26*, TC5003, doi:10.1029/2006TC002007.

Papanikolaou, D. J. (1984), The three metamorphic belts of the Hellenides. A review and a kinematic interpretation, *Geol. Soc. London, Spec. Publ.*, *17*(1), 551–561, doi:10.1144/GSL.SP.1984.017.01.42.

Papanikolaou, I. D., G. P. Roberts, and A. M. Michetti (2005), Fault scarps and deformation rates in Lazio–Abruzzo, Central Italy: Comparison between geological fault slip-rate and GPS data, *Tectonophysics*, *408*(1–4), 147–176, doi:10.1016/j.tecto.2005.05.043.

Papanikolaou, I. D., M. Foumelis, I. Parcharidis, E. L. Lekkas, and I. G. Fountoulis (2010), Deformation pattern of the 6 and 7 April 2009, MW = 6.3 and MW = 5.6 earthquakes in L'Aquila (Central Italy) revealed by ground and space based observations, *Nat. Hazards Earth Syst. Sci.*, *10*(1), 73–87, doi:10.5194/nhess-10-73-2010.

Pirazzoli, P. A. (1986), Marine notches, in *Sea-Level Research*, edited by Orson van de Plassche, pp. 361–400 , Springer, Dordrecht, Netherlands.

Pirazzoli, P. A., and N. Evelpidou (2013), Tidal notches: A sea-level indicator of uncertain archival trustworthiness, *Palaeogeogr. Palaeoclimatol. Palaeoecol.*, *369*, 377–384, doi:10.1016/j.palaeo.2012.11.004.

Pirazzoli, P. A. (1991) *World Atlas of Holocene Sea-Level Changes*, *Elsevier Oceanogr. Ser*, vol. 58, pp. 88–104, Elsevier, Amsterdam, New York.

Pirazzoli, P. A., J. Thommeret, Y. Thommeret, J. Laborel, and L. F. Montag-Gioni (1982), Crustal block movements from holocene shorelines: Crete and Antikythira (Greece), *Tectonophysics*, *86*(1–3), 27–43, doi:10.1016/0040-1951(82)90060-9.

Pirazzoli, P. A., L. F. Montaggioni, J. F. Saliège, G. Segonzac, Y. Thommeret, and C. Vergnaud-Grazzini (1989), Crustal block movements from Holocene shorelines: Rhodes Island (Greece), *Tectonophysics*, *170*(1–2), 89–114, doi:10.1016/0040-1951(89)90105-4.

Pirazzoli, P. A., J. Laborel, J. F. Saliège, O. Erol, İ. Kayan, and A. Person (1991), Holocene raised shorelines on the Hatay coasts (Turkey): Palaeoecological and tectonic implications, *Mar. Geol.*, *96*(3–4), 295–311, doi:10.1016/0025-3227(91)90153-U.

Pirazzoli, P. A., S. C. Stiros, M. Arnold, J. Laborel, F. Laborel-Deguen, and S. Papageorgiou (1994), Episodic uplift deduced from Holocene shorelines in the Perachora Peninsula, Corinth area, Greece, *Tectonophysics*, *229*(3–4), 201–209, doi:10.1016/0040-1951(94)90029-9.

Porter, N. J., A. S. Trenhaile, K. Prestanski, and J. I. Kanyaya (2010), Patterns of surface downwearing on shore platforms in eastern Canada, *Earth Surf. Process. Landforms*, *35*(15), 1793–1810, doi:10.1002/esp.2018.

Queffeulou, P., and A. Bentamy (2007), Analysis of wave height variability using altimeter measurements. Application to the Mediterranean Sea, *J. Atmos. Ocean. Technol.*, *24*(12), 2078–2092, doi:10.1175/2007JTECH0507.1.

Roberts, G. G., N. J. White, and B. Shaw (2013), An uplift history of Crete, Greece, from inverse modeling of longitudinal river profiles, *Geomorphology*, *198*, 177–188, doi:10.1016/j.geomorph.2013.05.026.

Roberts, G. P., S. L. Houghton, C. Underwood, I. Papanikolaou, P. A. Cowie, P. van Calsteren, T. Wigley, F. J. Cooper, and J. M. McArthur (2009), Localization of Quaternary slip rates in an active rift in 10 5 years: An example from central Greece constrained by 234 U-230 Th coral dates from uplifted paleoshorelines, *J. Geophys. Res.*, *114*, B10406, doi:10.1029/2008JB005818.

Rust, D., and S. Kershaw (2000), Holocene tectonic uplift patterns in northeastern Sicily: Evidence from marine notches in coastal outcrops, *Mar. Geol.*, *167*(1–2), 105–126, doi:10.1016/S0025-3227(00)00019-0.

Sakellariou, D., V. Lykousis, S. Alexandri, H. Kaberi, G. Rousakis, P. Nomikou, P. Georgiou, and D. Ballas (2007), Faulting, seismic-stratigraphic architecture and late Quaternary evolution of the Gulf of Alkyonides Basin? East Gulf of Corinth, Central Greece, *Basin Res.*, *19*(2), 273–295, doi:10.1111/j.1365-2117.2007.00322.x.

Schildgen, T. F., D. Cosentino, B. Bookhagen, S. Niedermann, C. Yıldırım, H. Echtler, H. Wittmann, and M. R. Strecker (2012), Multi-phased uplift of the southern margin of the Central Anatolian plateau, Turkey: A record of tectonic and upper mantle processes, *Earth Planet. Sci. Lett.*, *317-318*, 85–95, doi:10.1016/j.epsl.2011.12.003.

Schneiderwind, S., S. J. Boulton, I. Papanikolaou, and K. Reicherter (2017), Innovative tidal notch detection using TLS and fuzzy logic. Implications for palaeo-shorelines from compressional (Crete) and extensional (Gulf of Corinth) tectonic settings, *Geomorphology*, *283*, 189–200, doi:10.1016/j.geomorph.2017.01.028.

Serpelloni, E., C. Faccenna, G. Spada, D. Dong, and S. D. P. Williams (2013), Vertical GPS ground motion rates in the Euro-Mediterranean region: New evidence of velocity gradients at different spatial scales along the Nubia-Eurasia plate boundary, *J. Geophys. Res. Solid Earth*, *118*, 6003–6024, doi:10.1002/2013JB010102.

Sivan, D., S. Wdowinski, K. Lambeck, E. Galili, and A. Raban (2001), Holocene sea-level changes along the Mediterranean coast of Israel, based on archaeological observations and numerical model, *Palaeogeogr. Palaeoclimatol. Palaeoecol.*, *167*(1–2), 101–117, doi:10.1016/S0031-0182(00)00234-0.

Sivan, D., K. Lambeck, R. Toueg, A. Raban, Y. Porath, and B. Shirman (2004), Ancient coastal wells of Caesarea Maritima, Israel, an indicator for relative sea level changes during the last 2000 years, *Earth Planet. Sci. Lett.*, *222*(1), 315–330, doi:10.1016/j.epsl.2004.02.007.

Stewart, I., and C. Vita-Finzi (1996), Coastal uplift on active normal faults: The Eliki fault, Greece, *Geophys. Res. Lett.*, *23*(14), 1853–1856, doi:10.1029/96GL01595.

Stewart, I. S., A. Cundy, S. Kershaw, and C. Firth (1997), Holocene coastal uplift in the taormina area, northeastern sicily: Implications for the southern prolongation of the calabrian seismogenic belt, *J. Geodyn.*, *24*(1–4), 37–50, doi:10.1016/S0264-3707(97)00012-4.

Stiros, S. C., J. Laborel, F. Laborel-Deguen, S. Papageorgiou, J. Evin, and P. A. Pirazzoli (2000), Seismic coastal uplift in a region of subsidence: Holocene raised shorelines of Samos Island, Aegean Sea, Greece, *Mar. Geol.*, *170*(1–2), 41–58, doi:10.1016/S0025-3227(00)00064-5.

Stocchi, P., G. Spada, and S. Cianetti (2005), Isostatic rebound following the Alpine deglaciation: Impact on the sea level variations and vertical movements in the Mediterranean region, *Geophys. J. Int.*, *162*(1), 137–147, doi:10.1111/j.1365-246X.2005.02653.x.

Tortorici, L., C. Monaco, C. Tansi, and O. Cocina (1995), Recent and active tectonics in the Calabrian arc (southern Italy), *Tectonophysics*, *243*(1–2), 37–55, doi:10.1016/0040-1951(94)00190-K.

Torunski, H. (1979), Biological erosion and its significance for the morphogenesis of limestone coasts and for nearshore sedimentation (northern Ardriatic), *Senckenberg. Marit.*, *11*, 193–265.

Trenhaile, A. S. (2014), Modelling tidal notch formation by wetting and drying and salt weathering, *Geomorphology*, *224*, 139–151, doi:10.1016/j.geomorph.2014.07.014.

Trenhaile, A. S. (2015), Coastal notches. Their morphology, formation, and function, *Earth Sci. Rev.*, *150*, 285–304, doi:10.1016/j.earscirev.2015.08.003.

Trenhaile, A. S. (2016), Modelling coastal notch morphology and developmental history in the Mediterranean, *Geo. Res. J.*, *9-12*, 77–90, doi:10.1016/j.grj.2016.09.003.

Trenhaile, A. S., and D. W. Mercan (1984), Frost weathering and the saturation of coastal rocks, *Earth Surf. Process. Landforms*, *9*(4), 321–331, doi:10.1002/esp.3290090405.

Westaway, R. (1993), Quaternary uplift of southern Italy, *J. Geophys. Res.*, *98*(B12), 21,741–21,772, doi:10.1029/93JB01566.

Westaway, R., M. Pringle, S. Yurtmen, T. Demir, D. Bridgland, G. Rowbotham, and D. Maddy (2004), Pliocene and Quaternary regional uplift in western Turkey: The Gediz River terrace staircase and the volcanism at Kula, *Tectonophysics*, *391*(1–4), 121–169, doi:10.1016/j.tecto.2004.07.013.

Wöppelmann, G., and M. Marcos (2012), Coastal sea level rise in southern Europe and the nonclimate contribution of vertical land motion, *J. Geophys. Res.*, *117*, C01007, doi:10.1029/2011JC007469.

Zazo, C., P. G. Silva, J. L. Goy, C. Hillaire-Marcel, B. Ghaleb, J. Lario, T. Bardají, and A. González (1999), Coastal uplift in continental collision plate boundaries: Data from the last interglacial marine terraces of the Gibraltar Strait area (south Spain), *Tectonophysics*, *301*(1–2), 95–109, doi:10.1016/S0040-1951(98)00217-0.

Zazo, C., J. L. Goy, C. J. Dabrio, T. Bardají, C. Hillaire-Marcel, B. Ghaleb, J.-Á. González-Delgado, and V. Soler (2003), Pleistocene raised marine terraces of the Spanish Mediterranean and Atlantic coasts: Records of coastal uplift, sea-level highstands and climate changes, *Mar. Geol.*, *194*(1–2), 103–133, doi:10.1016/S0025-3227(02)00701-6.